

Environmental Research Center Papers

NUMBER 9

1986

Environmental Research Center
The University of Tsukuba

EXPERIMENTAL STUDIES ON TRANSIENT BEHAVIOR OF CAPILLARY ZONE*

By Abdul Khabir ALIM**

(received February 26, 1986)

ABSTRACT

In the analysis of the groundwater flow problems in unconfined aquifers, by considering the water table as the upper boundary of the flow system, the flow above the water table including the capillary zone was neglected until very recent years. On the other hand, when analyzing the unsaturated flow problems, the soil physicists consider the water percolation in the vadose zone (including the capillary zone) in vertical direction. Beside these problems, in subsurface flow studies, it is usually observed that the discharge rate and the water table position fluctuate during the rainfall events.

To investigate these problems, laboratory experiments were performed on Toyoura standard sand. The models for these experiments consist of a sand tank model, rainfall simulator and the ponding equipments. To analyze the behavior of flow in the capillary zone due to the water table movements, initial drying and boundary wetting experiments were conducted. For the investigations of the behavior of flow in the capillary zone due to the infiltration process, the rainfall and ponding infiltration experiments were carried out.

While performing the experiments under the water table movement, it was observed that with the development of suction in the outlet zone of the flow system, the upper boundary of the saturated capillary zone was acting as the upper boundary of the flow region. Moreover, during these experiments, it was found that the saturated capillary zone acts as a siphon for the water movement above the water table. Thus the capillary siphon flow concept was realized as a physically existing phenomenon.

On the other hand, when the behavior of capillary zone in response to infiltration was studied, it was found that the water in the vadose zone moved vertically down to the upper boundary of the saturated capillary zone. Therefore, the upper boundary of saturated capillary zone carries significant characters in subsurface flow studies.

Further it was clearly noticed that if the entrapped pore-air is compressed downward by the infiltrating water, the entrapped pore-air pressure gradually builds up to the air entry value of that soil material. At the final pressure build-up stage, the entrapped pore-air escapes from the soil profile and thereafter the flow system acts as an unconfined one with regard to the pore-air pressure build-up. During the entrapped pore-air pressure build-up, the water table and the discharge rate rise temporarily. This leads to understand that the entrapped pore-air is one of the main causes of pulsation in the discharge rate, the water table position and in the pressure head of the soil water systems. To reveal such a transient behavior, certain time is required for the displaced pore-air to become continuous in the soil profile. Eventually the time required for this purpose depends on the soil type, the boundary conditions of the flow system, the rainfall intensity and its duration.

*A dissertation submitted in partial fulfillment of the requirements for the degree of Doctor of Science in Hydrology to the Institute of Geoscience, the University of Tsukuba

**Address: P.O. Box 147, Kabul, Afghanistan (from April 1, 1986)

CONTENTS

ABSTRACT	1
LIST OF FIGURES	4
LIST OF TABLES	6
LIST OF SYMBOLS	7
CHAPTER I INTRODUCTION	8
1.1 General aspects	8
1.2 The role of infiltration in hydrological cycle	8
1.3 The role of capillary zone in groundwater flow studies	8
1.4 Previous studies	9
1.4.1 Physical aspects	9
1.4.2 Theoretical aspects	11
1.4.3 Practical aspects	14
1.5 Objectives	14
CHAPTER II EXPERIMENTAL APPARATUS AND PROCEDURE	15
2.1 Apparatus and instrumentations	15
2.2 Experimental procedure	18
2.3 Observed data	19
2.4 Physical properties of the soil medium	24
CHAPTER III DEFINITIONS AND PHYSICAL PROPERTIES OF THE CAPILLARY ZONE	25
3.1 Classification of zones above the water table	25
3.2 Physical properties of the capillary zone	25
3.3 Basic assumptions	26
3.4 Siphon flow action of the capillary zone	26
3.4.1 Initial drying process	26
3.4.2 Boundary wetting process	29
3.4.3 Quantitative analysis	33
3.5 Definition of terms used in this study	34
CHAPTER IV ENTRAPPED AIR AS A CAUSE OF PULSATION IN SUBSURFACE FLOW PHENOMENA	36
4.1 General aspects	36
4.2 The influence of capillary zone location on the subsurface flow behavior	36
4.3 The behavior of pressure head in a pulsating flow system	42

4.4	The behavior of flow in a pulsating flow system	47
4.5	Quantitative analysis	51
4.6	Discussion	53
CHAPTER V FLOW BEHAVIOR IN THE VICINITY OF SEEPAGE FACE		56
5.1	General aspects	56
5.2	The behavior of flow at the open face of the capillary zone	56
5.2.1	Due to the rainfall infiltration	56
5.2.2	Due to the ponding infiltration	56
5.3	Characteristics of flow in the seepage face	61
5.3.1	Due to the rainfall infiltration	61
5.3.2	Due to the ponding infiltration	62
5.4	Quantitative analysis	63
5.5	Discussion	66
CHAPTER VI DISCUSSION		67
6.1	Mechanism of pulsation in subsurface flow systems	67
6.2	Pore-air pressure effects at the open face of a subsurface flow system	68
6.3	Water table characteristics in the presence of vertical flow	68
6.4	The significance of air and water entry values in subsurface flow	70
6.5	Problems to be studied further	70
CHAPTER VII CONCLUSIONS		71
ACKNOWLEDGEMENTS		72
BIBLIOGRAPHY		73

LIST OF FIGURES

FIGURE	PAGE
2.1 Schematic diagram of the sand tank model	15
2.2 Schematic diagram of the rainfall simulator	16
2.3 Schematic diagram of the ponding facilities	18
2.4 Water Characteristic curve for Toyoura standard sand	24
3.1 Hydraulic condition of the sand tank at 37 minutes of the drying experiment	27
3.2 Hydraulic condition of the sand tank at 83 minutes of the drying experiment	28
3.3 Hydraulic condition of the sand tank at 136 minutes of the drying experiment	28
3.4 Discharge hydrograph of the sand tank during the drying experiment	29
3.5 Hydraulic condition of the sand tank at 47 minutes of the wetting experiment	30
3.6 Hydraulic condition of the sand tank at 217 minutes of the wetting experiment	31
3.7 Hydraulic condition of the sand tank at 541 minutes of the wetting experiment	31
3.8 Discharge hydrograph of the sand tank during wetting experiment	32
4.1 Combination of the discharge hydrographs for <i>EXPS. NO. 4</i> and <i>8</i>	37
4.2 Water table changes during <i>EXP. NO. 4</i>	38
4.3 Water table changes during <i>EXP. NO. 8</i>	38
4.4 Combination of the discharge hydrographs for <i>EXPS. NO. 5</i> and <i>9</i>	39
4.5 Water table changes during <i>EXP. NO. 9</i>	40
4.6 Combination of the discharge hydrographs for <i>EXPS. NO. 11</i> and <i>17</i>	40
4.7 Water table changes during <i>EXP. NO. 11</i>	41
4.8 Pressure head variations during <i>EXPS. NO. 4</i> and <i>8</i>	42
4.9 Pressure head variations during <i>EXPS. NO. 5</i> and <i>9</i>	43
4.10 Pressure head variations during <i>EXP. NO. 6</i>	43
4.11 Pressure head variations during <i>EXPS. NO. 11</i> and <i>17</i>	44
4.12 Pressure head profiles for the inlet zone, the middle and the outlet zone of the sand tank during <i>EXPS. NO. 4</i> and <i>8</i>	45
4.13 Pressure head profiles for the inlet zone, the middle and the outlet zone of the sand tank during <i>EXPS. NO. 11</i> and <i>17</i>	46
4.14 Flow patterns for <i>EXP. NO. 4</i> at 35 minutes	47
4.15 Flow patterns for <i>EXP. NO. 4</i> at 115 minutes	48
4.16 Flow patterns for <i>EXP. NO. 4</i> at 430 minutes	49
4.17 Flow patterns for <i>EXP. NO. 4</i> at 490 minutes	49
4.18 Flow patterns for <i>EXP. NO. 4</i> at 730 minutes	50
4.19 Flow patterns for <i>EXP. NO. 8</i> at 100 minutes	50

FIGURE	PAGE
4.20 Flow patterns for <i>EXP. NO. 8</i> at 390 minutes	51
4.21 Pore-air pressure build-up during <i>EXP. NO. 4</i>	53
5.1 Flow patterns for <i>EXP. NO. 11</i> at 30 minutes	57
5.2 Flow patterns for <i>EXP. NO. 11</i> at 100 minutes	58
5.3 Flow patterns for <i>EXP. NO. 11</i> at 460 minutes	59
5.4 Hydraulic condition of the sand tank at 40 minutes of <i>EXP. NO. 17</i>	59
5.5 Hydraulic condition of the sand tank at 100 minutes of <i>EXP. NO. 17</i>	60
5.6 Hydraulic condition of the sand tank at 240 minutes of <i>EXP. NO. 17</i>	60
5.7 Flow diagram of the seepage face during <i>EXP. NO. 4</i>	61
5.8 Flow diagram of the seepage face during <i>EXP. NO. 8</i>	62
5.9 Flow diagram of the seepage face during <i>EXP. NO. 11</i>	62
5.10 Schematic representation of the water balance for <i>EXP. NO. 4</i>	64
5.11 Schematic representation of the water balance for <i>EXP. NO. 8</i>	64
5.12 Schematic representation of the water balance for <i>EXP. NO. 11</i>	65
5.13 Schematic representation of the water balance for <i>EXP. NO. 17</i>	65
6.1 Water content variations in the inlet zone, the middle and outlet zone of the sand tank during <i>EXP. NO. 4</i>	69

LIST OF TABLES

TABLE		PAGE
2.1	Summary of the results of rainfall infiltration experiments	20
2.2	Summary of the results of ponding infiltration experiments	22
3.1	Summary of the flow net analysis for initial drying experiment	33
3.2	Summary of the flow net analysis for boundary wetting experiment	34
4.1	Summary of the flow net analysis for <i>EXP. NO. 4.</i>	52
5.1	Summary of the flow net analysis for <i>EXP. NO. 8.</i>	63
5.2	Summary of the flow net analysis for <i>EXP. NO. 11.</i>	63

LIST OF SYMBOLS

SYMBOL	DEFINITION
A	Cross-sectional area
B	Constant
C	Constant
H	Total potential
H_w	Depth of ponded water
h	Pressure head
h_{cr}	Critical pressure head
I_t	Accumulated infiltration
i	Hydraulic gradient
K	Hydraulic conductivity
K_s	Saturated hydraulic conductivity
L_f	Depth of the wetting front
Q	Discharge
S	Sorptivity
t	Time
v_f	Final infiltration rate
v_i	Infiltration rate
v_o	Initial infiltration rate
z	Elevation head
α	Constant
β	Constant
θ	Water content

CHAPTER I

INTRODUCTION

1.1 General aspects

The resultant force of the mutual attraction (cohesion) between water molecules themselves and the molecular attraction (adhesion) between water and different solid material raises the water among the non-solid space of a soil profile (Heath, 1983). This results the development of a capillary zone above the water table.

Generally, the capillary zone is influenced by the transient impacts of water table alteration as well as due to the infiltration or the percolation of surface water toward the groundwater bodies. The transient behavior of this zone caused by the water table alterations was investigated using one-dimensional column and two-dimensional sand tank models in a previous study (Alim, 1983). The results were further reported in detail by Alim and Kayane (1983; 1985). Brief results of the two-dimensional sand tank model studies, however, will be presented in Chapter III. This thesis deals with the above concept, but mostly due to the infiltration process, especially caused by the pore-air compression that affects the hydrological aspects of a subsurface flow system.

1.2 The role of infiltration in hydrological cycle

The existence of a hydrological cycle was thought of by Greek philosophers as early as in the fourth century. However the quantitative measurements of its main elements were not practiced until the late 17th century. Among the main elements of the hydrological cycles, the infiltration process plays significant roles on the formation of soil moisture profile, the overland flow generation, groundwater recharge, water table rise, soil erosion, and on the transport of pollutants to the groundwater reservoirs.

Although there is no clear distinction between percolation and infiltration in the literature, generally the term infiltration refers to the entry of water at the soil-air interface and percolation to the movement of water through the soil profile to the saturated zone.

When water enters into a soil profile, certain amount of infiltrated water is retained in the soil pores due to the capillary forces, but the excess water percolates downward by the gravity. The retained water in the soil profile plays an important role in the ecosystem as well as on the economy and the human welfare of the society (Dunne and Leopold, 1979, p. 126). On the other hand, the gravity percolated water reaches the saturated stratum of the soil profile and recharges the groundwater bodies that accounts for the two thirds of the fresh water resources of the world (Freeze and Cherry, 1979, p. 5).

1.3 The role of capillary zone in groundwater flow studies

For the analysis of saturated-unsaturated groundwater flow problems, a knowledge of the unsaturated flow and the gradual drainage or wetting of the pores is required. However this information is seldom available, especially in engineering applications. Hence in such cases, the flow through the unsaturated portion of the system is usually assumed to be negligible. Under this assumption the upper boundary of the flow system becomes the water table and the water table itself as a flow line (Freeze and Cherry, 1979, p. 188).

Nevertheless Muskat (1937, p. 372) and Akiba (1938) demonstrated that this assumption is not valid and the zone above the water table may act as a siphon in the direction of the main flow. Chapman (1960), Bouwer (1964), Schmid and Luthin (1964), Luthin (1969), Freeze (1971) and Vaucline *et al.* (1979), stated that the saturated hydraulic conductivity can be used for the region of uniform moisture content above the water table. In other words, this zone, *i. e.*, the capillary zone can be included as a part of the saturated zone. When the capillarity effect is ignored, it might be dependent on the ratio of the capillary rise to the average depth of the flow region (Chapman, 1960).

In actual circumstances, the flow in the saturated zone of the unconfined aquifers is analyzed by the Dupuit-Forchheimer's (D-F's) theory based on the assumption of horizontal flow. This method has been suggested by Bear (1979, p. 77) as a good approximation in regions where the slope of water table are indeed small, or the flow is horizontal. When considering the horizontal flow in a system, the vertical component of flow developed partly by the capillary potential is realized as negligible. This makes the theory an ideal one and sets limitations for application in practice. Kirkham (1967) discussed the paradoxes and some limitations were found on its applications by Bouwer (1965) and Willard and Monkmeyer (1973).

On the other hand, the flow of water in the vadose zone is often analyzed by using the unsaturated flow equation based on the capillary conductivity and the mass conservation law. But this equation traces the flow of water in this zone in vertical direction up the top of the water table. Basically the flow in the saturated zone below the water table is slow and moves in a laminar condition. Moreover, because of the small hydraulic conductivity of the unsaturated soil, the water movement in the vadose zone should be also slow. But when investigating the role of groundwater in storm runoff, Sklash and Farvolden (1979) reported the occurrence of large groundwater components in the runoff by the environmental isotope study. Therefore, the considerable contribution of groundwater with the discharge makes it necessary to investigate the role of the vadose zone, especially of the capillary zone in subsurface flow concept in detail.

1.4 Previous studies

The subject of infiltration has received great attention by the engineers and scientists in literature. However limited works are performed on its influences on the capillary zone. Here some of the studies related to the physical, theoretical and the practical aspects of infiltration will be reviewed.

1.4.1 Physical aspects

The physical aspects of infiltration are one of the most complicated subjects in hydrology, because of the displacement of pore-air by the infiltrating water in a soil profile. For this reason, the infiltration process has been known as a two-phase immiscible displacement phenomenon. To investigate this subject, understanding the physics of both fluids, *i. e.*, water and air is required. Information about the former fluid is available to some extent, but very scarce about the latter. Philip (1969) investigated this concept in detail, but provided little information on the condition of the displaced pore-air.

For a long time, it was believed that when infiltrating water enters into the soil profile, the air escapes through the unfilled water pores to the atmosphere (Youngs and Peck, 1964). This may be true if the capillarity is neglected in the flow process. Now it is clear that the infiltration

of water in a soil profile is accomplished by both, the capillarity and the gravitational forces (Rodda *et al.* 1976). In soil profiles with initial water content close to the irreducible water saturation, Noblanc and Morel-Seytoux (1972) found that the infiltration rate is very high during the first three hours of infiltration because of the capillarity. Consequently, due to the hysteretic behavior of capillary flow phenomenon, the argument of free escape of pore-air during infiltration is highly questionable.

During an infiltration process, a soil profile undergoes the following processes;

- a – the moisture content of the soil profile is subjected to certain changes,
- b – an equal amount of air to the infiltrated water must be removed from the soil,
- c – the exchange of place between air and water is accompanied by the development and dissipation of energy.

a – Soil moisture development during infiltration

The moisture development in a soil profile was classified by Vachaud *et al.* (1974) in the following three stages;

The first stage is the beginning of infiltration when the air can escape through the soil surface. As infiltration continues, a zone of high moisture content (wetting front) develops at the surface of the soil. The downward movement of the wetting front produces a compression of pore-air in the lower soil layers. By assuming a vertical flow, with uniform moisture content and hydraulic conductivity in the wetted zone, the infiltration process is analyzed as a piston flow (Bouwer, 1978, p. 253). The physics of piston flow however is not yet verified completely.

The second stage begins when the pore-air pressure near the soil surface becomes greater than the air entry value. At this stage some air flow occurs through the soil surface to the atmosphere. After this, the air phase is no longer confined in the porous domain.

The last stage occurs when the infiltrated water reaches the water table. This stage is often called as the redistribution process.

Nevertheless Philip (1957c) identified 5 zones in a soil column during an infiltration process. They are the saturated zone at the top followed by the transition, transmission, wetting zones and the wetting front. Among the others, Horton and Hawkins (1965) described the path of water movement, Childs (1967) and Knapp (1978) discussed the storage, and Vachaud and Thony (1971) explained the redistribution of water in the soil profile.

b – Behavior of air during infiltration

As mentioned earlier, by entering a certain volume of water into a soil profile, an equal amount of air must be displaced. However Wilson and Luthin (1963) reported that in homogeneous soils, the volume of air leaving the column exceeds the volume of infiltrating water.

Dixon and Linden (1972) in a border irrigation study characterized the condition of air in the soil as the displaced and the entrapped ones. They found that in the coarse porous media with large pores, the air pressure rises more rapidly than in fine media. Furthermore, they stated that the high intensity rains in the border and basin irrigations would develop displaced air pressure in large groundwater recharge basins. While the furrow, trickling sprinkler irrigations and the low intensity rainfalls would produce little or no air pressure. They emphasized that the soil-air pressure and its infiltration effects are not negligible as commonly ignored by the Darcy-based flow theory. For the interpretation of the soil-air pressure, they proposed a modified form of the

Boyle's law. But this method can be applied only for limited cases.

The significance of air compression in a soil profile due to infiltration has received great attention in literature. Among these, Bainchi and Haskell (1966) found that the apparent rise in water table prior to the arrival of the wetting front results from a localized response of the observation wells to pressure associated with the air movement between the water table and the wetting front. Vachaud *et al.* (1973; 1974) reported that it affects the advance of the wetting front. Touma *et al.* (1984) found that the air pressure decreases the water potential at the soil surface. This results the reduction of infiltration rate to about one-third of the value when the air is free to escape. Further, Parlange and Hill (1979) noticed that if the air flow is not restricted, hence the compressibility negligible, the air movement increases the water intake by increasing water pressure near the soil surface.

However, Morel-Seytoux (1978) observed that the effects of air compression are important only when the water contents are close to saturation over a particular portion of the soil profile. Corey (1977, p. 197) emphasized that at beginning when the initial saturation is substantially less than 1.00, the air resistance has little effect. But he stated that when saturation becomes bigger, the air pressure continues to rise to a critical threshold pressure value at which the air breaks through the surface.

McWhorter (1971) studied the significance of air in the infiltration process and found that the air begins to escape from the top of the column when the capillary pressure at the surface has reached to some threshold value. According to Bouwer (1966), the air entry value can be the closest approximation of critical pressure for the desorption. Nevertheless, Peck (1965) reported that the air pressure required to initiate air escape from a vertical bounded column could be equal to the minimum depth of the saturated zone plus the air entry value of the material.

In this context, the diffusion of trapped gas from the porous media was studied by Adam *et al.* (1969), and others. The methods for its measurement and for the determination of vertical air movement in the field are given by Debacker (1967) and Weeks (1978), respectively.

c — Energy development due to the air-water interchange

When water enters into a soil profile, some volume of air must be displaced. This interchange of water with the air is accompanied with the energy formation and dissipation. Philip (1959 a, b) explained that generally the heat released by viscous dissipation of energy will not be great enough to invalidate an isothermal process approximation during absorption and infiltration processes. Corey (1977, p. 194) mentioned that the viscous resistance to air flow due to infiltration may or may not be important. But Wilson and Luthin (1963) reported that the displacement of air by the water during an infiltration process is not isothermal. Anderson and Linville (1962) by monitoring the temperature at a localized site during the infiltration found that the temperature at any given point was rising gradually and then dropt sharply when the water approached and passed the measuring point.

1.4.2 Theoretical aspects

Since this research is an experimental one, the theoretical aspects are discussed here very short. The details of the theory as well as of the solutions of infiltration equations are given by Philip (1957a; b; 1985a; b; 1969), Bouwer (1964; 1969), Childs (1967), Noblanc and Morel-Sytoux (1972), Mein and Larson (1973), Morel-Seytoux and Khanji (1974), Brutsaert (1977), Collis-

George (1977) and Morel-Seytoux (1978). In this section, this subject is divided in the following order.

a – Infiltration Equations

The quantitative study of infiltration began more than 70 years ago when Green-Ampt (1911) derived the equation (Eq. 1.1) empirically.

$$v_i = K \frac{H_w + L_f - h_{cr}}{L_f} \dots \dots \dots (1.1)$$

where v_i : infiltration rate [L/T]
 K : hydraulic conductivity of the wetting zone [L/T]
 H_w : depth of water above soil [L]
 L_f : depth of wetting front [L]
 h_{cr} : critical pressure head [L]

Originally this approach was involved with ponding of water on the soil surface and based on the assumption of constant hydraulic conductivity and water content in the advancing wetting zone as well as constant (negative) pressure at the advancing front. Moreover, they assumed the existence of a distinct and precisely definable wetting front. However, when Swartzendruber (1974) applied this approach to the infiltration data obtained under constant rainfall intensity, the flux equations encountered difficulty.

Neuman (1976) described that the Green-Ampt concept is a piston displacement in which the vertical flux may change with time but not with elevation. Bouwer (1969) also emphasized that this model is similar to a piston flow, particularly valid for infiltration into a layered profile where K decreases with depth after the wetting. Moreover Corey (1977, p. 194) argued that this theory does not provide any information about the distribution of saturation with respect to depth and time.

Morel-Seytoux and Khanji (1974) pointed out that although the empirical parameters of this theory have a very precise physical meaning, the assumption of a front separating a saturated zone from the zone at initial water content can cause relative errors of prediction of 10 to 70%. However, Parlange (1975) expressed that the error resulting from the Green-Ampt equation is 20% at most for moderate times and gets even smaller as the pressure head increases.

Dixon (1976) in a comment stated that the Green-Ampt equation seems to be less suitable for application in applied hydrology than Kostiaikov's equation (Eq. 1.2).

$$I_t = C t^\alpha \dots \dots \dots (1.2)$$

where I_t : accumulated infiltration [L]
 t : time since the start of infiltration [L]
 C and α : constants

Because this equation expresses the infiltration rate I_t as a function of time instead of as a function of the wetting front depth. But Childs (1969, p. 279) expressed that Kostiaikov's equation may be valid only in the initial stages of infiltration and certainly not for longer periods.

The next infiltration equation referred in literature is the Horton's equation (Eq. 1.3).

$$v_i = v_f + (v_o - v_f) e^{-\beta t} \dots\dots\dots (1.3)$$

where v_o : initial value of the infiltration rate [L/T]
 v_f : final value of the infiltration rate [L/T]
 v_i : infiltration rate [L/T]
 β : constant

In this equation β is calculated from the field measurements. According to Bouwer (1978, p. 256) the disadvantage of Horton's equation is that theoretically $v_o = \infty$, so that a realistic value for v_o is difficult to select. Philip (1957d) pointed out that the final constant infiltration rate in the Horton's curve is numerically equivalent to the saturated hydraulic conductivity of the soil. This point was also emphasized by Freeze and Cherry (1979, p. 212) based on the Rubin *et al.* (1963; 1964) works.

Furthermore, Philip (1957d) introduced an equation for accumulated infiltration in the form of (Eq. 1.4).

$$I_t = S t^{1/2} + B t \dots\dots\dots (1.4)$$

where I_t : accumulated infiltration [L]
 S : sorptivity [L.T]
 t : time [T]
 B : constant

Philip explained how to estimate the value of the constant (B), used in this equation. Peck (1965) applied this equation to calculate the time length that the effect of gravity in pore-air pressure can be neglected.

b – Theoretical analysis

Infiltration of water into porous media such as soil, is analyzed as an unsaturated flow. Quantification of the flow during this process is performed by Richard's (1931) equation derived from the combination of the differential form of the Darcy's law with that of the mass conservation. Details of the derivation as well as introducing the specific moisture capacity and the diffusivity in one-dimensional form of this equation were explained in a previous study (Alim, 1983).

Philip (1957a) described the initial and boundary conditions required for the analysis of groundwater movement (wetting or the drainage) with the infiltration or evaporation process in an unsaturated soil based on this equation. Freeze (1969) provided a review of the available numerical solutions for one-dimensional vertical, unsaturated, unsteady flow problems in tabular form. Among the others, recently by using the Richard's equation, a general solution to infiltra-

tion process is done by Warrick *et al.* (1985). Nevertheless, Mein and Larson (1973) and others stated that this equation is not suitable for general application, but it is considered to be the best method available for computing the vertical flow of soil moisture.

Two-dimensional analysis of the infiltration problems are given by numerous researchers, *e. g.*, Brutsaert (1971), and Perrens and Watson (1977). The two-phase infiltration problems were analyzed by Brutsaert and Morel-Seytoux (1970) and others. Unsteady rainfall was studied by Morel-Seytoux *et al.* (1977) and Chu (1978) and the response of water table with series of rainfall events has been investigated by Rennolls *et al.* (1980) and Stephens and Neuman (1982).

1.4.3 Practical aspects

Besides the facts that the infiltration process plays distinguished functions in our environment, some of the natural deficiencies also can be adjusted artificially by using this process. Among these, to use the physical effects of the entrapped pore-air on the soil profile caused by the infiltration, the following points can be mentioned.

Since the entrappment of air in the soil profile reduces the infiltration rates, Dixon and Linden (1972) demonstrated that the rate and the route of water penetration into the soil can be controlled by regulating the displaced air pressure. On the other hand, they emphasized that the infiltration could be increased by cultural practices designed to reduce the build up of the displaced air pressure. In contrast Philip (1969) argued that in flooded regions, the developed soil air pressure is great enough to lift the pavements of highways.

1.5 Objectives

In this experimental study it is tried to investigate the significances that a capillary zone carries in response to the saturated and unsaturated flows. It will also be attempted to make clear the effects of the entrapped pore-air on the subsurface flow phenomena. Particularly the following subjects are considered as the objectives of this study.

- 1 – To study the transient response of the subsurface hydrological phenomena with regard to the integrated saturated-unsaturated flow.
- 2 – To clarify the siphon flow action of the capillary zone due to the water table movements.
- 3 – To elucidate the transient impacts of infiltration on the pore-air pressure condition of an unsaturated soil.
- 4 – To make clear the importance of pore-air condition on the discharge and on the water table positions when the capillary zone is located at different distances from the ground surface.
- 5 – To find whether in transient condition, the open face of the capillary zone to the atmosphere in a hydrological system act as a seepage face when the pore-air pressure of the system increases by the advancing wetting front.

CHAPTER II

EXPERIMENTAL APPARATUS AND PROCEDURE

2.1 Apparatus and instrumentations

The models used in this research are consisting of the sand tank model, the rainfall simulator and the ponding equipments.

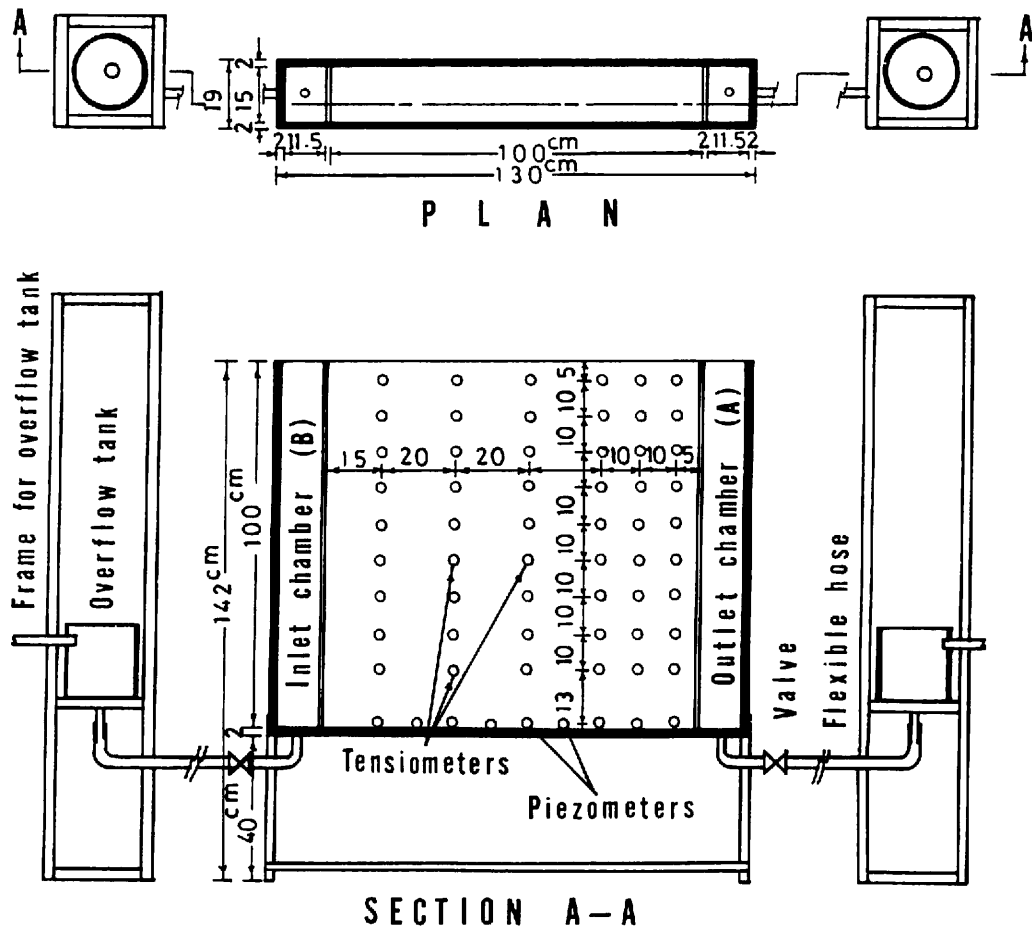


Fig. 2.1 Schematic diagram of the sand tank model.

The sand tank model shown in Fig. 2.1 is composed of a sand tank, two water level controlling overflow tanks, and a manometer board. The sand tank is made from acrylic transparent plates with 130 cm length, 15 cm width and 100 cm height. At the two ends of the sand tank, the inlet and the outlet chambers, each with 11.5 cm width are located. To control the water level in these

chambers, each of them is connected with one water level controlling overflow tank. The water level controlling overflow tanks are made from P.V.C. pipes with 125 mm diameter and 20 cm height. They are equipped with one outlet at the base and one overflow pipe at 15 cm from the base. The overflow tanks are connected with the sand tank by the water hoses.

For the measurements of total potential at various parts of the sand tank, 54 tensiometers were fixed in 6 columns and in 9 rows on one side of the tank. At the lowest part of the sand tank 9 piezometers were installed at 10 cm in horizontal distances. The locations of the tensiometers and the piezometers are shown in Fig. 2.1.

The walls separating the inlet and the outlet chambers from the main part of the sand tank are 10 mm thick plastic plates. For the filtration experiments under the confined pore-air pressure condition, these plates are perforated up to 50 cm height from the bottom. Above this level they were sealed against air and water escape. But for the unconfined pore-air pressure infiltration as well as for the groundwater table alteration experiments, these walls were completely permeable. For the measurements of water table inside the sand tank, 4 observation pipes were installed at 3, 33, 66 and 97 cm distances from the inlet boundary.

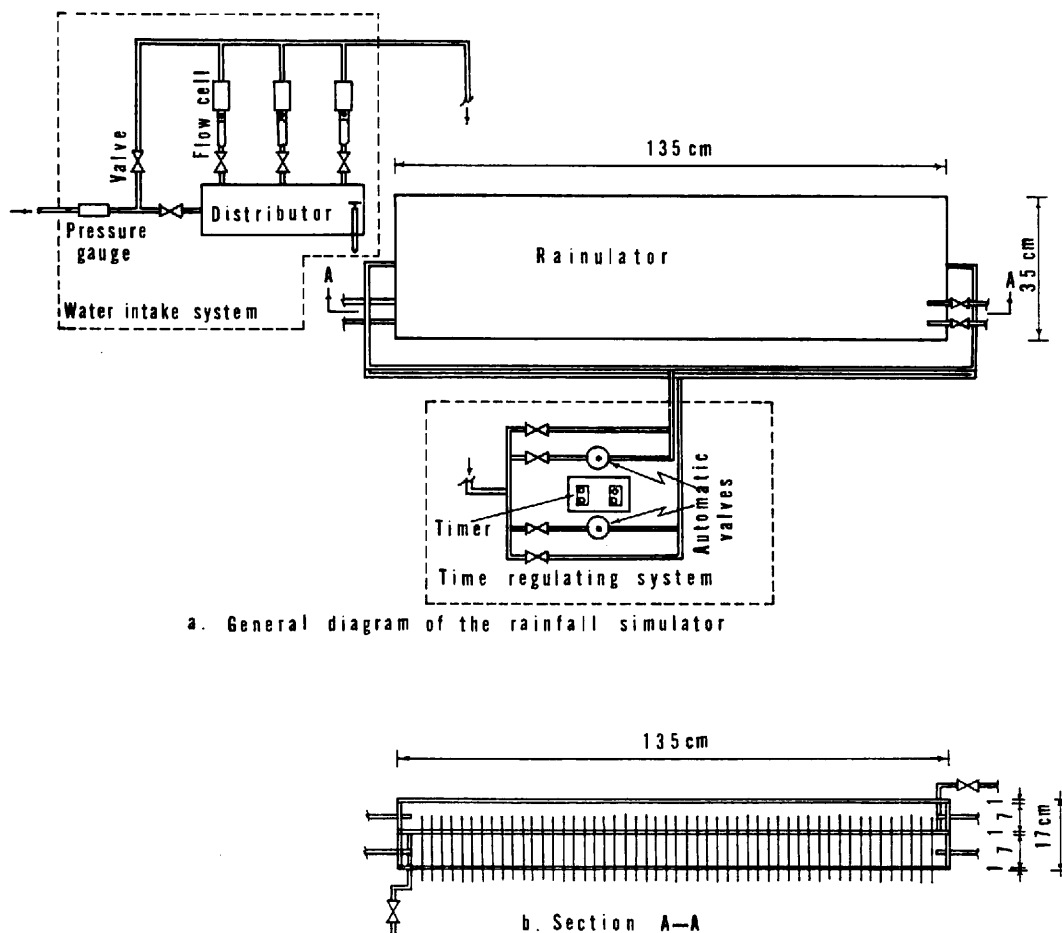


Fig. 2.2 Schematic diagram of the rainfall simulator.

The artificial rainfall simulator shown in Fig. 2.2 consists of a water intake regulating system, the automatic time regulating system and the rainulator itself. The water intake regulating system is made of a distributor, measuring flow cells and a by-pass line. The distributor is made of 125 mm P.V.C. pipe 40 cm in length. It is equipped with one inlet, one overflow and three outlet pipes each 13 mm inside diameter. The three outlet lines are connected with three high pressure flow cells ranging from 0.6 to 4, from 2 to 15 and from 4 to 30 lit/hr capacity respectively. In this manner, it is possible to run the experiments within the range of 0.6 to 49.0 lit/hr.

The rainulator is made of acrylic transparent plates with 135 cm length, 35 cm width and 19 cm height. It is composed of two compartments, the upper and the lower, each with 7 cm height. There are 663 stainless needles with 0.7 mm inside diameter inserted into the rainulator to produce the rain drops. These needles are 8 and 16 cm long inserted alternatively to the lower and the upper compartments. The distance between the needles in each compartment is 5 cm. Hence the rainfall drops on the sand bed at 2.5 cm intervals. To supply water in these compartments, the line coming from the water intake regulating system is divided into two parts each connected with the lower and the upper compartments of the rainulator.

The rainulator is made into two compartments to regulate the rain drops falling over the sand bed in such a way that they do not fall continuously at one point, but in an alternating manner. For this purpose the supply lines of the compartment are equipped each with one automatic valve operated by an electric timer. The rainulator is placed over a frame able to move over and away from the sand tank.

The ponding equipment shown in Fig. 2.3 is consisting of a ponding reservoir and a constant head elevated tank. The ponding reservoir is made of acrylic transparent plates 100 cm long, 15 cm wide and 15 cm of height.

The constant head elevated tank is also made of transparent plates. A pipe with 125 mm diameter and 15 cm height is fixed at the middle of the constant head tank to serve as an overflow tank. The overflowing water is drained from this tank by a drain pipe.

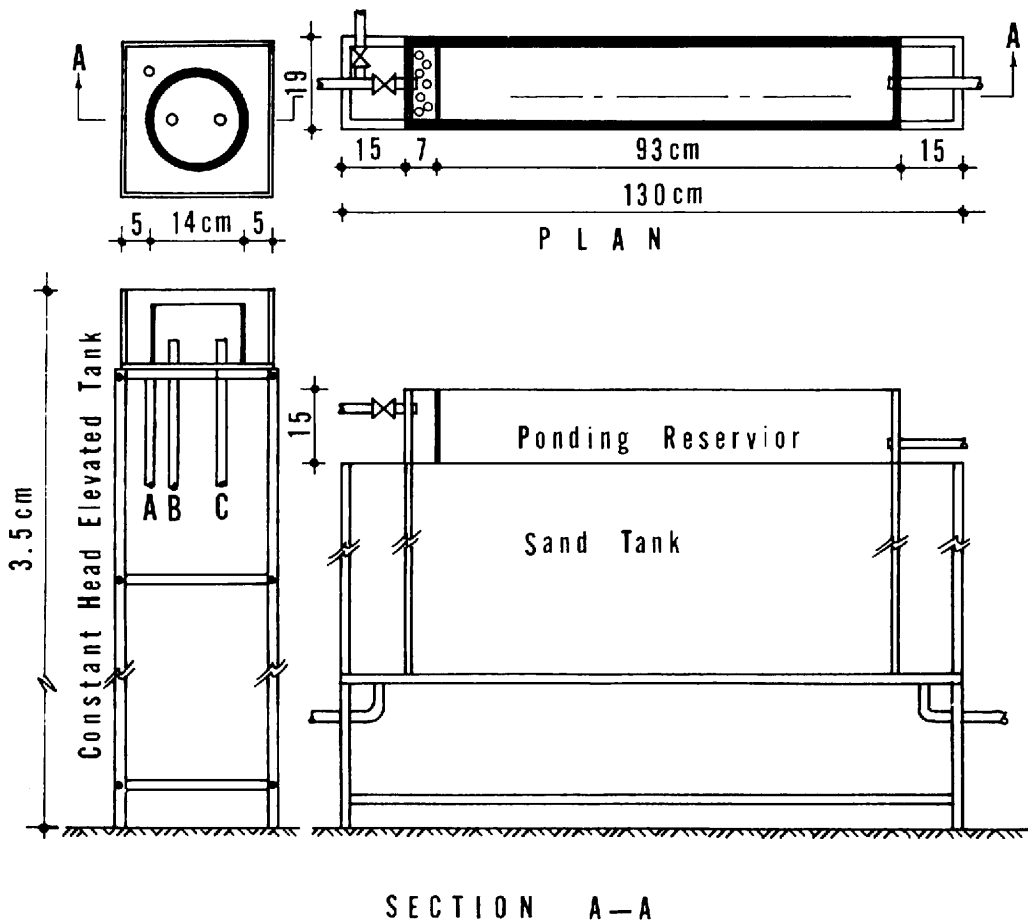


Fig. 2.3 Schematic diagram of the ponding facilities.

2.2 Experimental procedure

A homogeneous sand filling of the tank was accomplished by pouring de-aired water to a certain height in the sand tank followed by filling the sand inside the water and tamping it with the rod. After 2–5 days from sand filling, the water table inside the sand tank was lowered in 6 steps, namely, 5, 20, 20, 15, 10 and 5 cm by lowering the water level in the outlet chamber both for the confined and the unconfined infiltration experiments. After each water level drops in the outlet chamber, the sand tank was allowed to drain at least for 24 hours.

2.2.1 Confined infiltration experiments

At the beginning the water table was fixed at 80 cm level below the sand surface in which the upper boundary of the capillary zone reaches to 25 cm from the sand surface. At this condition the rainfall infiltration experiments were performed under various rainfall intensities and durations (EXPS. NO. 1–4 of Table 2.1).

The water table was raised to 55 cm level from the sand surface. In this case the upper boundary of the capillary zone reaches the sand surface. At this condition *EXP. NO. 5* (Table 2.1) was performed. The water table was raised again to 20 cm position below the sand surface in order to perform experiments when the upper boundary of the saturated capillary zone (for the definitions, see Chapter III) coincides with the sand surface. Under this condition *EXP. NO. 6* was conducted.

After the rainfall infiltration experiments, the ponding reservoir was fixed over the sand tank and the ponding infiltration experiments of this series (*EXPS. NO. 10 to 15* in Table 2.2) were performed under different water table locations and different ponding depths. The boundary conditions as well as a brief summary of the results of all the experiments are given in Tables 2.1 and 2.2.

2.2.2 Unconfined infiltration experiments

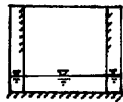
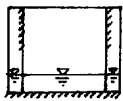
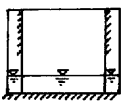
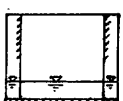
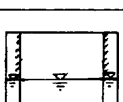
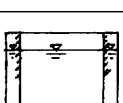
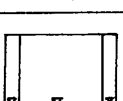
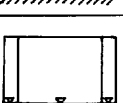
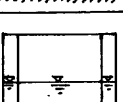
To conduct this series of experiments, sand was taken out of the tank. After oven-drying, it was packed again as for the confined infiltration experiments. At the beginning, the water table was fixed at 80 cm level below the sand surface by lowering the water level in the outlet chamber in 6 steps as explained before. Rainfall infiltration experiments of this series were followed by the ponding infiltration experiments.

2.3 Observed data

From each experiment explained above, the total potential, water table locations, the amount of inflow and the outflow, the excess flow for water level controlling (during ponding experiments under unconfined pore air pressure condition) and the overland flow in the case of ponding infiltration experiments were recorded in appropriate time intervals.

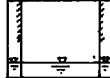
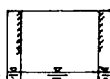
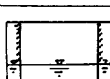
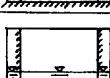
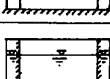
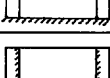
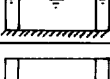
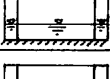
A total number of 17 experiments were performed for this study. They are consisting of 6 confined, 3 unconfined rainfall, 6 confined and 2 unconfined ponding infiltration experiments. In this thesis, however, the results of 7 experiments, namely, 3 confined and 2 unconfined rainfall, one confined and one unconfined ponding infiltration experiments will be presented. The experiments that their results are discussed here are marked as (*) in Tables 2.1 and 2.2.

Table 2.1 SUMMARY OF THE RAINFALL INFILTRATION EXPERIMENTS

Exp. No.	Boundary Conditions		Rainfall Intensity	Rainfall Duration	Discharge Started After	Maximum Discharge	Maximum Water Table Rise
			mm/hr	mins.	min.	ml/sec	cm
1	2	3	4	5	6	7	8
1			60.3	180	23.0	2.49	11.0
2			60.3	480	19.0	2.70	11.0
3			100.0	360	23.0	4.3	19.4
4 *			100.0	900	24.0	5.2	19.5
5 *			100.1	900	11.0	4.01	11.0
6 *			96.5	200	2.7	3.6	10.5
7			60.3	600	36.0	3.24	12.9
8 *			110.0	960	26.0	4.81	21.9
9 *			108.6	900	4.0	4.58	13.8

Maximum Pressure Head at Sand Surface	Maximum Length of Seepage Face	Average Rate of Discharge	Remarks
cm of H ₂ O	cm	ml/sec	
9	10	11	12
-32.0	1.0	2.34	
	1.5	2.60	
	3.0	3.87	-The discharge and the water table rise were in pulsating manner.
-25.0	3.5	4.21	-Around 480 minutes the discharge, water table positions as well as the pressure head rised to the maximum value, then reduced and continued in a rather less pulsating manner.
-21.6	1.0	3.9	-After 3 hours of rainfall a sudden decrease in potential was observed and the discharge also reduced by about 0.5 ml/sec.
+3.0			-After 20 minutes ponding took place and the overland flow was combined with the sub-surface flow, no exact measurement of sub-surface discharge was possible.
-28.4		2.77	
-26.0	1.5	4.56	
-24.7	1.0	4.35	-Only one significant rise in discharge and the water table position was observed around 270 minutes, but mostly it was not fluctuating considerably.

Table 2.2 SUMMARY OF THE PONDING INFILTRATION EXPERIMENTS

Exp.	Boundary Condition	Ponding Type	Average Depth of Ponding	Ponding Duration	Discharge Started After	Maximum Discharge	Maximum Water Table	Maximum Pressure Head at Sand Surface
			cm	min	min	ml/sec	cm	cm of H ₂ O
1	2	3	4	5	6	7	8	9
10		IR. T.	8.4	1020	11.0	15.53	49.0	-0.1
11*		IN. T.	6.5	600	1.5	12.70	47.0	+1.5
12		IR. T.	9.6	615	4.5	9.67	33.6	+3.4
13*		IN. T.	10.9	730	1.83	8.87	34.4	+2.4
14		IN. T.	11.5	500	0.83	5.58	13.2	+1.4
15		IN. T.	8.4	375	1.75	11.26	17.7	+0.5
16		IN. T.	0.5	480	2.3	17.53	72.0	+4.5
17*		IN. T.	10.3	480	2.5	24.1	72.0	-0.2

Maximum Length of Seepage Face	Average Rate of Discharge	Average Rate of Overland	Average Rate of Inflow	Percentage of Discharge to total Flow	Remarks
cm	ml/sec	ml/sec	ml/sec	%	
10	11	12	13	14	15
5.0	14.21	5.88	20.09	70.7	-Air escape was observed alternatively. -Water was flowing from 7 cm above the water level of the outlet chamber like a pipe flow.
5.0	12.33	1.20	13.4	91.0	-Air escape was observed alternatively for 407 minutes. -Water was flowing from all parts of the outlet boundary up to 8 cm above water level in the outlet chamber.
1.5	8.5	9.65	18.15	46.8	-Air escape was observed for 214 minutes but after this no air escape was seen.
2.5	8.21	6.06	14.27	57.5	-When water was poured on the sandbed, a continuous air escape was observed for 12 minutes. -At the beginning discharge was in great quantity that some was spoiled.
2.0	4.52	12.97	17.49	25.8	-No air escape was observed till the end, but air bubbles were observed at the sand surface.
2.5	10.05	4.78	14.83	67.8	-The groundwater mound produced at the beginning was existing till the end.
	17.28	0.00	17.7	100	-Water level in the inlet chamber was controlled at a constant elevation. -No overland flow took place.
5.0	22.93	0.92	32.72	99.0	-Water level in the inlet chamber was controlled at a constant elevation. The quantity of overflowing water from inlet chamber was 9.6 ml/sec.

2.4 Physical properties of the soil medium

The soil used in these experiments was Toyoura standard sand (a commercial sand type in Japan) with 0.16 mm effective diameter, specific gravity of 2.66, saturated hydraulic conductivity of 0.0144 cm/sec and 44% porosity. The water characteristic curve for this sand obtained by one-dimensional column experiments (Alim and Kayane, 1983) is given in Fig. 2.4. The methods for the determination of these properties as well as the procedure for the column experiments are given elsewhere (Alim, 1983).

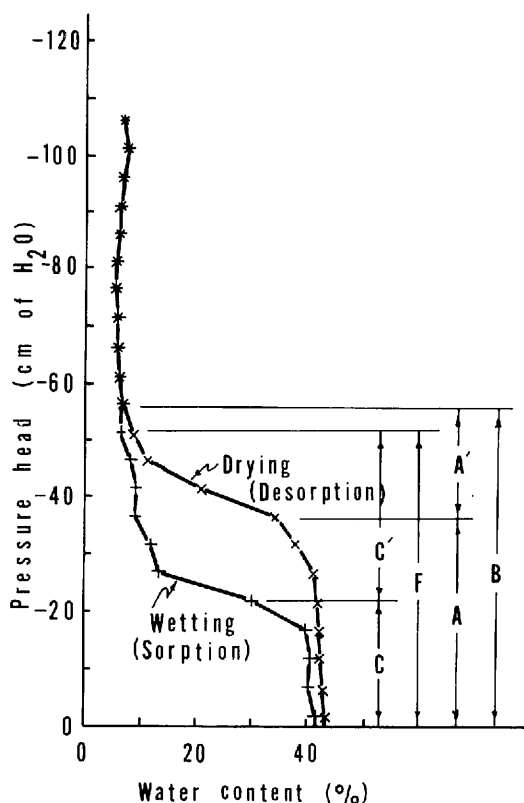


Fig. 2.4 Water characteristic curve for Toyoura standard sand.

- A : Saturated capillary zone (drying)
- A' : Unsaturated capillary zone (drying)
- B : Capillary zone in the drying cycle
- C : Saturated capillary zone (wetting)
- C' : Unsaturated capillary zone (wetting)
- F : Capillary zone in the wetting cycle.

CHAPTER III

DEFINITIONS AND PHYSICAL PROPERTIES OF THE CAPILLARY ZONE

3.1 Classification of zones above the water table

From the water content measurements and the total potentials response with regard to the water table alteration performed by the one-dimensional column experiments reported by Alim and Kayane (1983), the zone above the water table during the sorption and the desorption processes was divided into the capillary and the residual water saturation zones.

Using Figure 2.4, the *B* zone of the desorption and the *F* zone of the sorption cycles are the drying and the wetting capillary zones. The difference in heights of these zones indicates the hysteric behavior of the soil water phenomenon.

B zone of the desorption cycle is divided into the *A* and *A'* zones. In the same way, the *F* zone of the sorption cycle is divided into the *C* and *C'* zones. *A* and *C* zones are called as the saturated capillary zone, while *A'* and *C'* zones as the unsaturated capillary zones.

3.2 Physical properties of the capillary zone

From the classification of zones above the water table in previous section, some physical characteristics of these zones are described in this section.

It is clear from Fig. 2.4 that the water contents in the *A* and *C* zones are nearly the same as the water content in the saturated zone below the water table. As a consequence, these two zones are found to be at quasi-saturation condition and connected with the zone below the water table through the interconnected pore water. When the water table fluctuates, the potential within these zones also changes simultaneously with the zone below the water table. This means that the total potential gradient in these zones through the whole desorption and the sorption processes is nearly zero as in the saturated zone.

Consequently, if the negative pressure of these zone is not considered, they can be thought as a part of the saturated zone and the same flux as in the saturated zone should be taken into consideration. This consideration coincides with many researchers results as reviewed in Section 1.3. It can be anticipated therefore that as the pneumatic potential of the vadose zone increases, the pressure of these zones may also be changed, sometimes to positive values. As Bouwer (1978, p. 27) reports, the evidences of positive pressure heads in the vadose zone have already been observed by the hydrologists. The pressure heads at the upper boundaries of the *A* zone in the desorption and the *C* zone in the sorption cycles coincides with the air and water entry values, respectively.

The *A'* and the *C'* zones in the desorption and the sorption curves are the zones in which the water content changes from point to point. In addition, the total potential gradient within these zones becomes zero after 2 days from the change of water table position, as in the *A* and *C* zones. Although the pores of the soil profile in the *A'* and *C'* zones are not saturated with water, they are connected with the saturated capillary zone as well as with the saturated zone below the water table through the interconnected film-water surrounding the outer surface of each soil particle. The upper boundaries of these zones determined from the total potential and water content variations indicate the upper influence range of the capillary rise in the soil profile. The detailed discussions on these zones are given by Alim and Kayane (1983; 1985).

The existing waters in the irreducible water saturation zone are not connected with each other as they are found at contact points in the soil profile. Consequently, the total potential response in the irreducible water saturation zone is also different from the capillary and the saturated zones.

3.3 Basic assumptions

Before presenting the results of the experiments, it is necessary to mention the basic assumptions considered for the experiment and data analysis.

- 1 – The sand bed is homogeneous and isotropic.
- 2 – The physical, chemical and biological properties of the soil and of the water remain constant during the experiment.
- 3 – Water moves in the soil pores only due to the hydraulic gradient.
- 4 – The temperature within the system remains constant.

3.4 Siphon flow action of the capillary zone

The siphon flow action of the capillary zone was studied under both, the initial drying (water table fall) as well as due to the boundary wetting (water table rise) experiments. The results of these experiments are discussed in the following sections.

3.4.1 Initial drying process

To make the model ready for carrying out the drying experiments, water table in the sand tank was adjusted at 54 cm position from the base by adjusting the water levels in the inlet and the outlet chambers. When equilibrium was assured, the overflow tank of side *A* (Fig. 2.1) was lowered by 10 cm, while the position of overflow tank at side *B* was remained unchanged. From the start of experiment, the total potentials were recorded at every 10 to 20 minutes time intervals and the amount of discharge was measured. This experiment was continued for consecutive 136 minutes.

The hydraulic condition of the sand tank at 37 minutes of this experiment is shown in Fig. 3.1. In this figure, the shapes of potential lines in the saturated capillary zone near the inlet boundary of the tank show the presence of upward fluxes. These fluxes indicate the migration of water from the saturated zone to the capillary zone through the water table. Conversely, near the outlet zone, the existing downward fluxes express entering of water to the saturated zone from the capillary zone. Thus the zone having fluxes with the upward components is known as the recharging area and the zone with the downward components as the discharging area of the capillary zone. At this time the recharging area of the capillary zone covers about 1/3 of the total surface area of the sand tank.

In connection with the recharging and the discharging areas, the discharge hydrograph (shown in Fig. 3.4), reveals that at 37 minutes of the experiment, the discharge rate is in a recovery condition from a considerable decrease. The discharge returns to normal for a while but again decreases with the reduction of pore water above the water table.

There is a slight difference in the hydraulic condition of the sand tank at 83 minutes shown in Fig. 3.2 than at 37 minutes. Although the water table at this time does not reach to a stable position, the shapes of potential lines in this figure reveal completion of the drainage from most of the pores above the water table.

By the drop of water table in a soil profile, the drainage of water from the pores in the vadose zone starts and continues until equilibrium interfaces of curvature develop in the soil pores

(Childs, 1969, p. 122). Since all the pores of a soil matrix are not uniform and their interfaces of curvature do not reach to equilibrium position at the same time, a complete drainage of pore water from a soil profile requires long time. However at this time also the water is taken from the saturated zone by the capillarity near the inlet boundary and released back near the outlet boundary of the sand tank.

At 136 minutes, the recharging area of the capillary zone (shown in Fig. 3.3) has changed slightly near the inlet boundary of the sand tank, but the potential lines near the outlet boundary are intensified than that of 83 minutes. The above mentioned fact shows that the flow developed at the early stages of the experiment within the saturated capillary zone is still continuing and this zone behaves as a siphon for water transport from the inlet to the outlet zones as demonstrated by Muskat (1937) and Akiba (1938).

The discharge hydrograph during this experiment is shown in Fig. 3.4. It can be seen that by the application of suction, the outflow starts immediately and reaches to the highest value within a short period (under this experimental condition in 4 minutes). But very soon it falls and continues until the end with fluctuations.

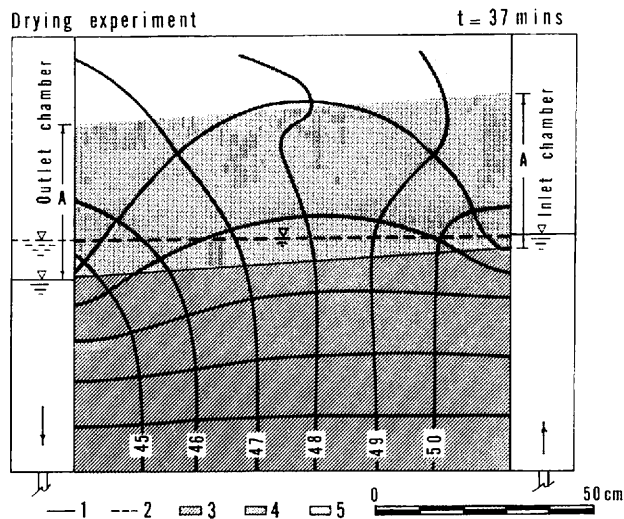


Fig. 3.1 Hydraulic condition of the sand tank at 37 minutes of the drying experiment.

- 1 : Water table position at 37 minutes;
- 2 : Water table position at initial condition;
- 3 : Saturated zone;
- 4 : Saturated capillary zone;
- 5 : Unsaturated capillary zone.

Note: Explanation for the A zone is given in Fig. 2.4.

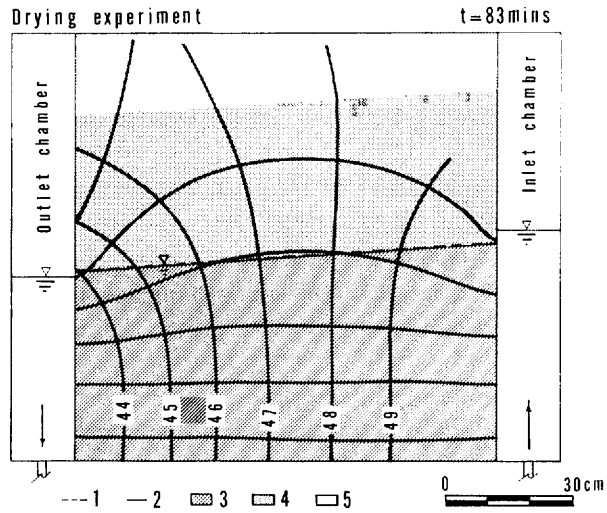


Fig. 3.2 Hydraulic condition of the sand tank at 83 minutes of the drying experiment.

- 1 : Water table position at 83 minutes;
- 2 : Water table position at 37 minutes;
- 3 : Saturated zone;
- 4 : Saturated capillary zone;
- 5 : Unsaturated capillary zone.

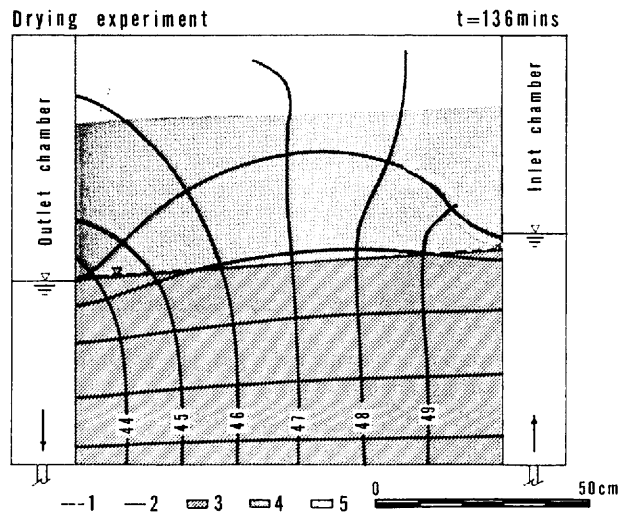


Fig. 3.3 Hydraulic condition of the sand tank at 136 minutes of the drying experiment.

- 1 : Water table position at 136 minutes;
- 2 : Water table position at 83 minutes;
- 3 : Saturated zone;
- 4 : Saturated capillary zone;
- 5 : Unsaturated capillary zone.



Fig. 3.4 Discharge hydrograph of the sand tank during the drying experiment.

3.4.2 Boundary wetting process

To make the model ready for the wetting experiment, the positions of both overflow tanks were adjusted at 24 cm levels from the base. When the hydraulic condition of the sand tank reached to equilibrium, the overflow tank of the *A* side (Fig. 2.1) was raised by 10 cm. The total potentials and the amount of discharge were recorded in appropriate times of the experiment. This experiment was conducted for consecutive 541 minutes.

The hydraulic condition of the sand tank at 47 minutes of this experiment is shown in Fig. 3.5. In this figure, as in the case of drying experiment, near the inlet zone of the sand tank the upward fluxes arising from the saturated zone toward the capillary zone can be observed. The directions of these fluxes are reversed, however, in downward direction near the outlet zone of the tank when they enter again into the saturated zone through the water table. Since in this case also the flow above the water table takes place within the saturated capillary zone, this zone is recognized as a siphon for water passage from the inlet to the outlet zones of the sand tank.

At this time, an advancing front of the capillary rise is generated at 55 cm above the initial water table position. Due to the rise of water table in a soil profile, the soil pores below the new position of water table are gradually filled under the influence of hydrostatic pressure. It is a gradual process, because all the pores can not be filled with water at the same time due to the differences in size of the soil-pores. Furthermore, above a rising water table, due to the presence of differences in attraction between portions of not equally moist soils, a driving force or the capillary current is produced (Baver, 1956, p. 227). At the beginning, because the vertical difference in moisture contents of the vadose zone is great between the points, the capillary activities are also strong and therefore an advancing front develops.

As the wetting process continues and more water is stored in the soil pores of the capillary zone, the differences in attraction becomes smaller. This results a reduction in capillary activities.

Consequently the hydraulic condition of the sand tank at 217 minutes shown in Fig. 3.6 apparently depicts the reduction in gradients of these upward fluxes. Finally, as shown in Fig. 3.7 by reaching the hydraulic condition of the sand tank at 541 minutes to equilibrium, this frontal zone disappears.

It is seen in the wetting process that the advancing front of capillary rise develops at the upper boundary of capillary zone, established before the change of water table position. Because in equilibrium condition all the forces present among the soil pores at this boundary are balancing each other. Moreover above this boundary, the zone with zero moisture gradient is present. By the start of the wetting process, the equilibrium of soil-water breaks and the capillary rise starts from this boundary. Consequently certain time is required for the process to restore the equilibrium condition here and form the new boundary at which all the forces among the soil pores balance each other.

In addition, it was observed that the saturated capillary zone either in the drying or in the wetting process acts as a siphon for water transport from the inlet to the outlet zones of the sand tank. This is because the saturated capillary zone is in quasi-saturation condition, *i. e.*, all the pores are nearly saturated with water. Therefore a continuity of pore-water exists between the saturated zone and the saturated capillary zone. In the case of drying, by lowering the water level in the outlet chamber, the drainage of water from the soil pores above the water table begins from the discharging area of the capillary zone and extends to the recharging area of this zone.

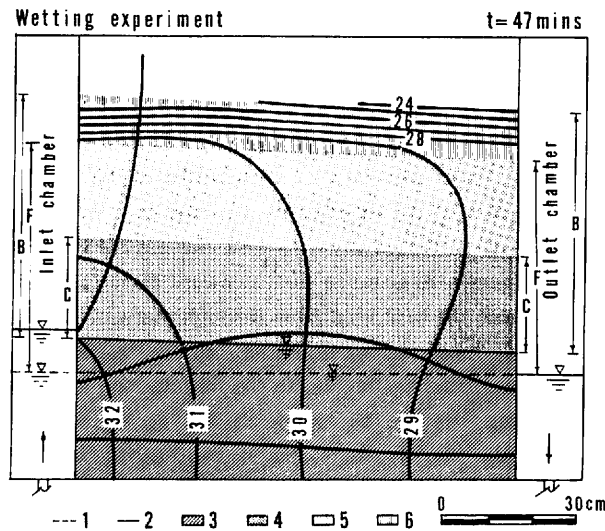


Fig. 3.5 Hydraulic condition of the sand tank at 47 minutes of the wetting experiment.

- 1 : Water table position at initial condition;
- 2 : Water table position at 47 minutes;
- 3 : Saturated zone;
- 4 : Saturated capillary zone;
- 5 : Unsaturated capillary zone;
- 6 : Advancing front of the capillary rise.

Note: Explanations for the B, C and F zones are given in Fig. 2.4.

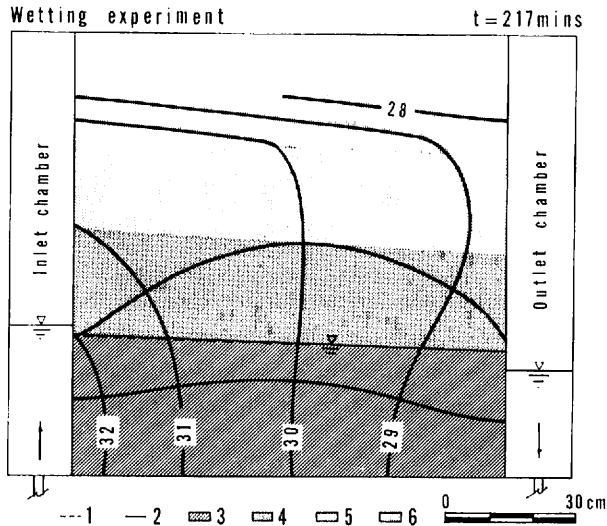


Fig. 3.6 Hydraulic condition of the sand tank at 217 minutes of the wetting experiment.

- 1 : Water table position at 47 minute;
- 2 : Water table position at 217 minutes;
- 3 : Saturated zone;
- 4 : Saturated capillary zone;
- 5 : Unsaturated capillary zone;
- 6 : Advancing front of the capillary rise.

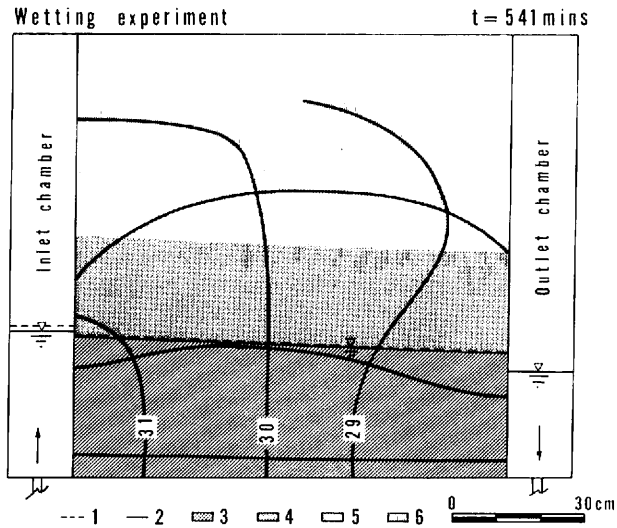


Fig. 3.7 Hydraulic condition of the sand tank at 541 minutes of the wetting experiment.

- 1 : Water table position at 217 minutes;
- 2 : Water table position at 541 minutes;
- 3 : Saturated zone;
- 4 : Saturated capillary zone;
- 5 : Unsaturated capillary zone;
- 6 : Advancing front of the capillary rise.

When water is transported from the recharging area to the discharging area of the capillary zone, the drained pores of the recharging area are subjected to hydraulically unequilibrium condition at that moment. As a result, surface tension forces become active and water is extracted from the saturated zone. On the other hand, due to the presence of suction at the outlet zone, the pores are drained of water simultaneously. Therefore, the water raised by the surface tension forces in the recharging area of the capillary zone gradually fills the drained pores of the outlet zone. In this way a siphon for water convey establishes and the water movement continues until the potential difference exists.

Conversely, as the water content in the unsaturated capillary zone is not close to the saturation water content, a continuity of pore water does not exist in this zone. Therefore, the drainage of pores near the outlet zone does not affect the conditions of the neighboring pores here. For this reason the path of water movement can not be established within this zone and the flow of water does not take place considerably.

In the wetting process also due to the presence of continuity in pore-water between the saturated zone and the saturated capillary zone, a siphon flow can be established. But in the unsaturated capillary zone since the pores are not filled with water completely, the siphon flow is not observed.

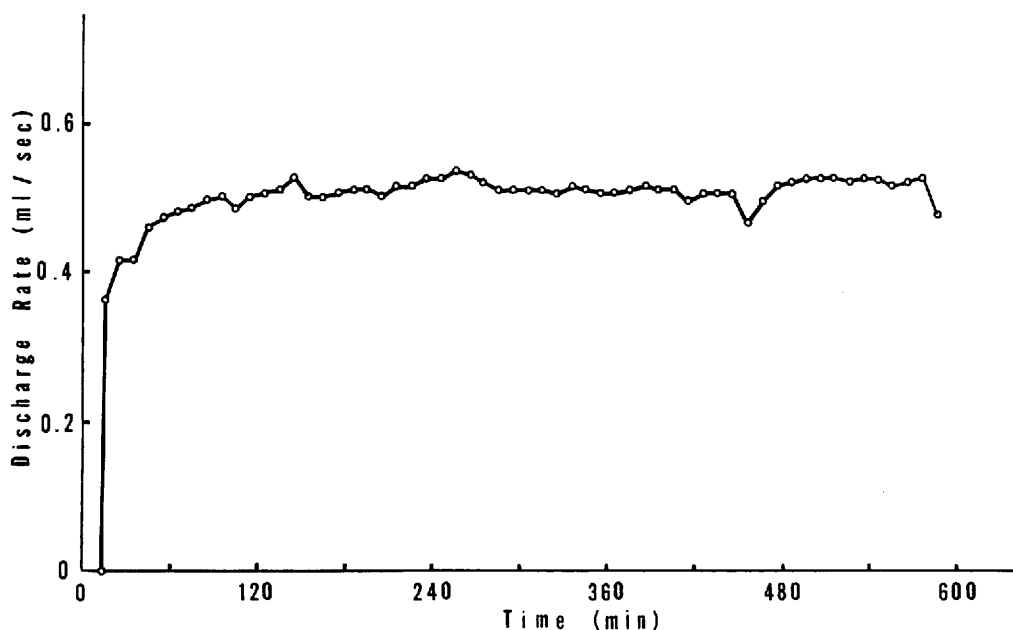


Fig. 3.8 Discharge hydrograph of the sand tank during the wetting experiment.

The condition of the discharge during this experiment is shown in Fig. 3.8. From this figure it is seen that under this experimental condition the discharge starts after 14 minutes. But in contrast with the drying experiment, it rises for about 90 minutes. After reaching the maximum value, it continues with minor fluctuations. These fluctuations in subsurface flow phenomenon in this study is called as the pulsation. The mechanism of pulsation of the discharge rate and the water table position will be discussed in Chapter VI.

3.4.3 Quantitative analysis

To determine the amount of flow below as well as above the water table during the drying and wetting experiments, the flow net analysis was performed on the potential distributions of the sand tank. For this purpose, the method for the flow net analysis described by Cedergren (1977) and McWhorter and Sunada (1977) was used. The values of hydraulic conductivities for the zone above the water table were obtained from the water content-pressure head relations of Fig. 2.4, using the Brooks and Corey's (1964) method. Since the values of water content for the saturated capillary zones in the desorption and sorption cycles are near the saturation water content, the values of unsaturated hydraulic conductivities for these zones come as the saturated hydraulic conductivity. This fact also has been emphasized by Chapman (1960) and Bouwer (1966).

Table 3.1 The amount of discharge calculated for the saturated, saturated capillary and the unsaturated capillary zones during the initial drying experiment

Time	Hydraulic Gradient	Saturated zone		Saturated capillary zone		Unsaturated Capillary Zone		Total		Measured Discharge
		Discharge	%	Discharge	%	Discharge	%			
min	m/m	ml/sec		ml/sec		ml/sec		ml/sec		ml/sec
37	0.068	1.23	65.0	0.63	33.5	0.02	1.1	1.88		1.90
83	0.068	1.06	69.7	0.45	29.6	0.01	0.7	1.52		-
136	0.068	1.16	68.2	0.53	31.2	0.01	0.6	1.7		-

The amount of discharge for the drying experiment was calculated using Figs. 3.1, 3.2 and 3.3 for 37, 83 and 136, minutes respectively. The result are summarized in Table 3.1. To realize the significances of the saturated, saturated capillary and unsaturated capillary zones in subsurface flow phenomena, the amount of discharge was calculated for each zone. It can be seen in the table that the amount of water flowing through the capillary zone is considerable at the early stages of the drying process. This is due to the presence of more recharging area of the capillary zone as well as the drainage water from the upper soil pores. Later as the drainage water from the above mentioned pores are reduced, furthermore, because the recharging area of the capillary zone contracts, *i. e.*, less water is extracted from the saturated zone below the water table, the amount of discharge reduces.

By using Figs. 3.5, 3.6 and 3.7, the amount of discharge was calculated for 47, 217 and 541 minutes of the wetting experiment, respectively. They are shown in Table 3.2. It is obvious from this table that at the beginning of a wetting process the amount of discharge is small. Because at this stage, more water is required to be stored in the capillary pores of the soil profile. Latter as the difference of moisture content in the saturated capillary zone becomes small, *i. e.*, little amount of the extracted water from saturated zone remain in the capillary pores, the amount of discharge also increases.

Table 3.2 The amount of discharge calculated for the saturated, saturated capillary and the unsaturated capillary zones during the wetting experiment

Time	Hydraulic	Saturated zone		Saturated Capillary zone		Unsaturated Capillary zone		Total	Measured
	Gradient	Discharge	%	Discharge	%	Discharge	%		Discharge
min	m/m	ml/sec		ml/sec		ml/sec		ml/sec	ml/sec
min	m/m								
47	0.039	0.27	58.7	0.19	41.3	0.00	0.0	0.46	0.47
217	0.039	0.31	58.5	0.22	41.5	0.00	0.0	0.53	0.52
541	0.039	0.31	58.5	0.22	41.5	0.00	0.0	0.53	0.52

A comparison of Tables 3.1 and 3.2 indicates that in places where the thickness of the saturated zone below the water table is small, the contribution of capillary zone to the discharge becomes great. Moreover, the hydraulic gradient produced in the drying experiment was 42% more than the wetting case. It is clear that due to the rise of water table in a soil profile, the flow in saturated zone is accompanied with smaller vertical component than due to water table drop. Consequently, as Willard and Monkmeyer (1973) remarked, for the unsteady case, the D-F's equation describes a rising water table more exactly than it does for a falling one.

3.5 Definition of terms used in this study

From the classification of soil profile above the water table made in previous section, the following definitions are used for the capillary zone in this study.

CAPILLARY ZONE: The zone above the water table in which water rises by the capillary forces. More specifically, the zone above the water table hydraulically connected through the tension-saturated pore-water (the zone with a uniform degree of saturation) and the film-water (the zone in which only the outer surface of the soil particles are covered with water) with the saturated zone below the water table.

SATURATED CAPILLARY ZONE: It is referred to that part of the vadose zone in which its lower boundary is the water table and its upper boundary coincides with the zone in which the pressure head is equivalent to the air entry (due to the water table fall) and the water entry (due to the water table rise) values of the soil profile. Moreover, the degree of saturation in the saturated capillary zone is uniform, i. e., $(d\theta/dz) = 0$, where θ is the water content, and z the distance above water table.

UNSATURATED CAPILLARY ZONE: It is a part of the vadose zone in which only the outer surface of the soil particles are covered with water and the degree of saturation differs from point

to point. The lower boundary of this zone is the zone in which the pressure head is equivalent to the air entry (due to the water table fall) or the water entry (due to the water table rise) values of the soil material. Its upper boundary reaches the irreducible water saturation zone.

Some other terms used in this thesis that may bring complications in the usage are defined as follows.

CONFINED PORE AIR PRESSURE (CPAP): This term is referred to the condition where the pore-air can escape only through the soil surface vertically to the atmosphere if the water content of the soil surface allow.

UNCONFINED PORE AIR PRESSURE (UCPAP): This term is referred to the condition where the pore-air can escape laterally as well as vertically through the soil surface to the atmosphere if the water content of the soil profile allow.

OVERLAND FLOW: The amount of water that can not infiltrate into the soil body and therefore flow through the ground surface to the down-stream of a watershed.

PIEZOMETRIC SURFACE: The height of the water level rising in a column of acrylic tube connected with the piezometer fixed in a soil body for the soil-water potential measurement.

CHAPTER IV

ENTRAPPED AIR AS A CAUSE OF PULSATION IN SUBSURFACE FLOW PHENOMENA

4.1 General aspects

It is widely observed that most of the subsurface flow in the field as well as in the laboratory investigations are accompanied with fluctuations spatially and quantitatively. Tanaka *et al.* (1982) monitored the occurrence of fluctuation in the outflow data of an experimental basin during a storm. They related, however, the fluctuation due to the soil piping.

In a previous study on the transient behavior of capillary zone due to the groundwater table alteration discussed in Chapter III, Alim (1983) observed the occurrence of pulsation in the discharge hydrographs. In the case of groundwater table alteration, in contrast with that of the pipe flow concept, the accumulation of water in the soil pores is accomplished by the gravitational and the capillary forces. Therefore in such cases the occurrence of pulsation in the flow is due to the presence of small hydraulic gradient to move the water constantly in the soil pores. Moreover, since the water movement in an unsaturated soil is accompanied by a continuous interchange of the water and air, the hysteresis of soil water can be the other cause of pulsation in subsurface flow phenomena.

In this chapter attempts have been made to clarify the significance of pore-air on the pulsation of the discharge rate, the water table position as well as on the pressure head in a soil profile.

4.2 The influence of capillary zone location on the subsurface flow behavior

To examine the effects of capillary zone location on the subsurface flow concept, the results of *EXPS. NO. 4, 5, 8, 9, 11* and *17* are presented and they are discussed in detail.

The combination of the discharge hydrographs for rainfall infiltration *EXP. NO. 4 (CPAP)* and *NO. 8 (UCPAP)* are given in Fig. 4.1. As explained earlier, these experiments were performed when the water table was located at 80 cm from the sand surface. In this case the upper boundary of the capillary zone reaches to 25 cm below the sand surface. The difference in the discharge rates in these figures is due to the difference in rainfall intensities of the experiments.

In this figure it is seen that in the case of the *CPAP* experiment (*EXP. NO. 4*), after about 420 minutes from the start, the discharge rate starts to rise from 4.2 ml/sec and reaches at 475 minutes to 5.18 ml/sec, an increase of 0.98 ml/sec within 55 minutes. After 475 minutes, the discharge rate at first drops rapidly but slowly later and continues till the cease of rainfall with minor fluctuations.

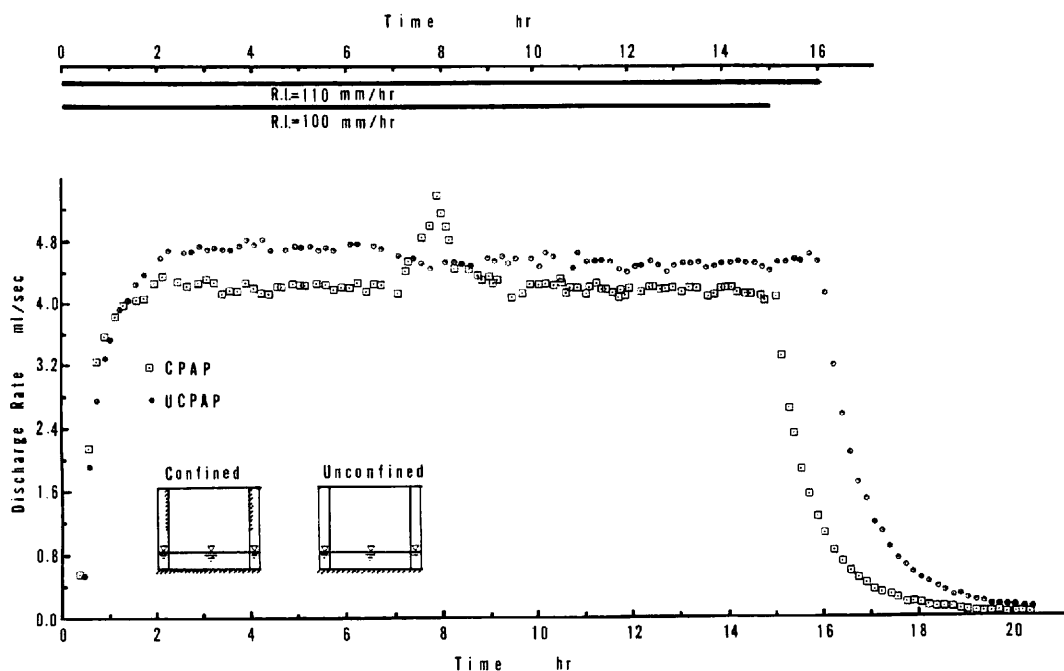


Fig. 4.1 Combination of the discharge hydrographs for *EXPS. NO. 4* and *8*.

When the pattern of the discharge rate is considered for the *UCPAP* experiment (*EXP. NO. 8*), it does not show great fluctuations, but there is relatively a large declination around 400 minutes. This declination of the discharge rate continues for about one hour. Afterward it takes a normal rate and continues with minor fluctuations until the cease of the rainfall. Moreover, during this experiment, the rises and the falls as well as the magnitude of fluctuations in the discharge rates occur in more or less at the same time as in the *CPAP* experiment.

The changes in the water table position during *EXPS. NO. 4* and *8* are shown in Fig. 4.2 and 4.3, respectively. As can be seen, the same characteristics are present here as in the discharge hydrograph of each experiment. During the *CPAP* experiment (*EXP. NO. 4*), the water table begins to rise at about 420 minutes and reaches around 480 minutes of the experiment to the highest value. Within this transient period, the water table rose about 3.5 cm higher than the position before 420 minutes. But the water table changes during the *UCPAP* experiment (*EXP. NO. 8*) did not show greater fluctuation. Furthermore, the water table during these experiments fluctuated at the same time as the discharge rate of each one experienced.

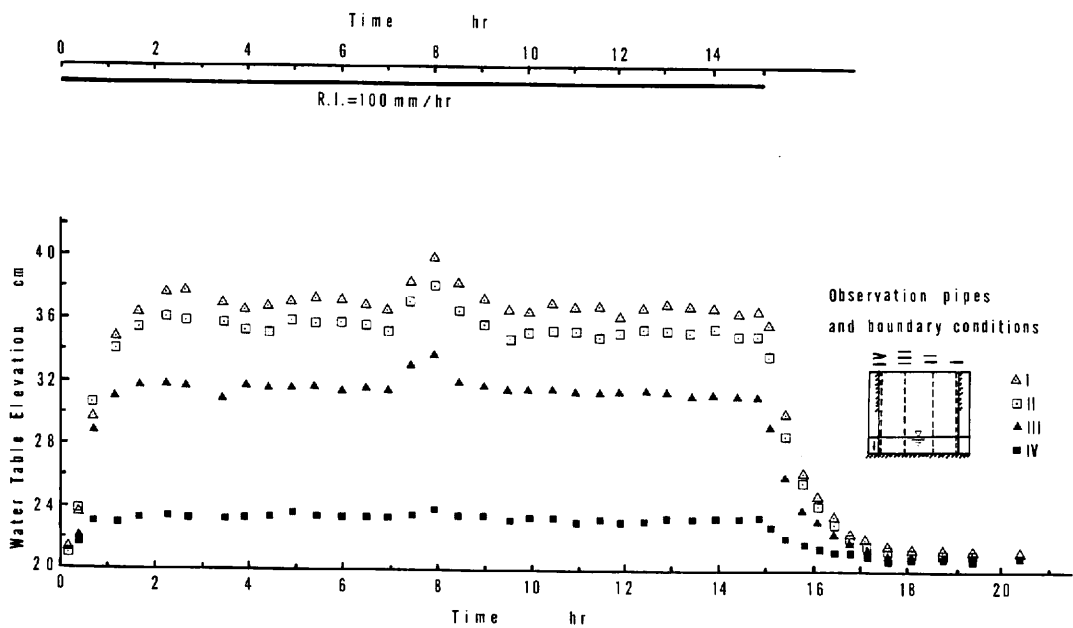


Fig. 4.2 Water table changes during *EXP. NO. 4*.

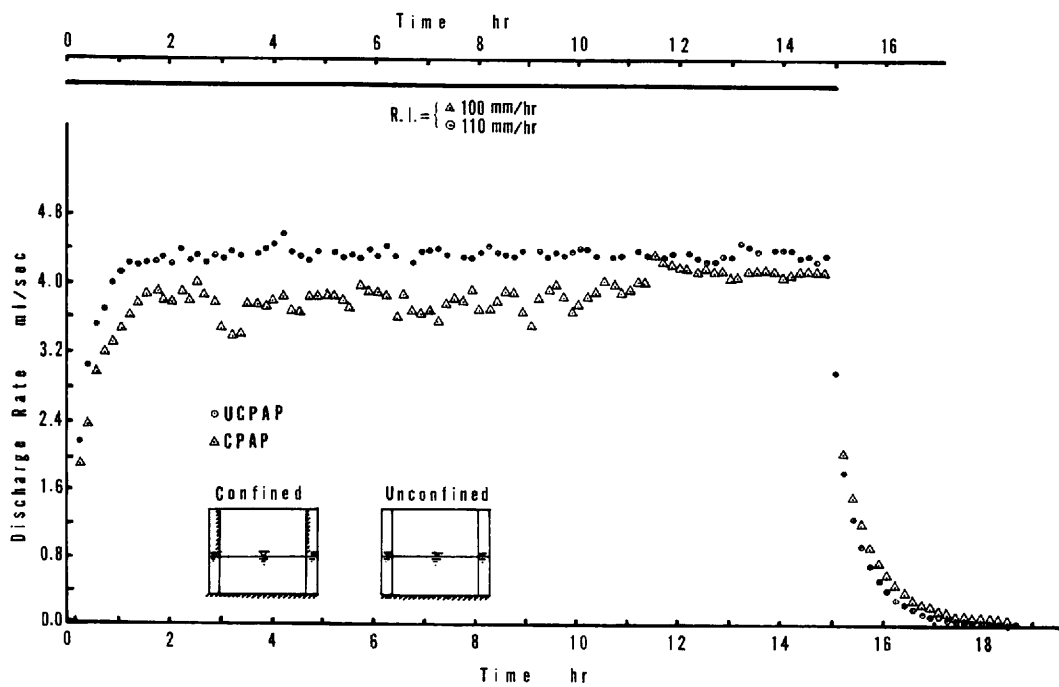


Fig. 4.3 Water table changes during *EXP. NO. 8*.

If the behavior of pulsation is studied during the *CPAP* and *UCPAP* experiments when the water table was initially located at 55 cm below the sand surface, (*EXPS. NO. 5* and *9*, respectively), different patterns of fluctuations are observed. In this case the upper boundary of the capillary zone coincides with the sand surface. The discharge hydrographs for these experiments are shown in Fig. 4.4. In this case also the differences in the discharge rates are due to the differences in the rainfall intensities. This figure shows that the number and the magnitude of fluctuations during the *CPAP* experiment are significant than the *UCPAP* experiment. Nevertheless, the time of rise in the discharge of one experiment coincides well with the other's fall.

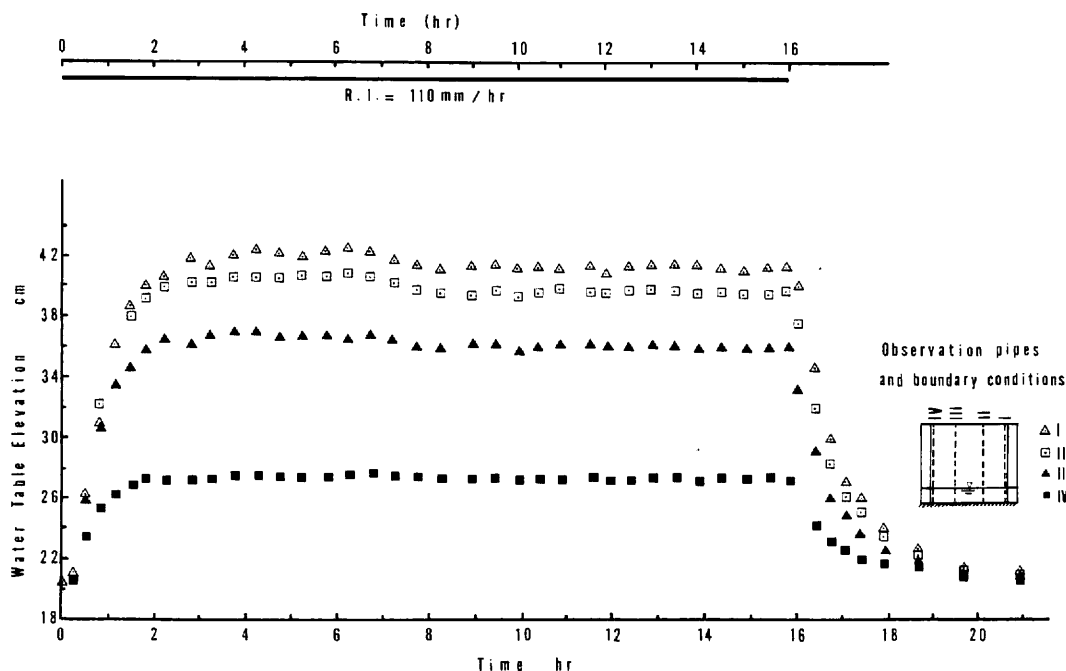


Fig. 4.4 Combination of discharge hydrographs for *EXPS. NO. 5* and *9*.

From the water table changes of these experiments, the one belonging to *EXP. NO. 9* is shown in Fig. 4.5. In this figure the pressure heads of the 5 cm layer below the sand surface are also presented. The smooth pattern of the water table changes without significant alteration is seen in this figure clearly. Moreover, the same fluctuations observed in the discharge rates and in the water table positions are also present with the pressure heads.

To examine the characteristics of pulsation in the discharge rate during the ponding infiltration process, the discharge hydrographs for the *CPAP* and the *UCPAP* ponding experiments, (*EXPS. NO. 11* and *17*, respectively), are illustrated in Fig. 4.6. In both cases the water table was located initially at 80 cm below the sand surface. To perform these experiments, a certain ponding depth was made on the sand surface by pouring water instantly. After that, this depth was maintained at a constant level by allowing an inflow of water. The excess water was drained in the form of overland flow out of the ponding reservoir. In this figure also the difference in the discharge rates are due to the differences in the amounts of inflow rates. The rate of inflow for

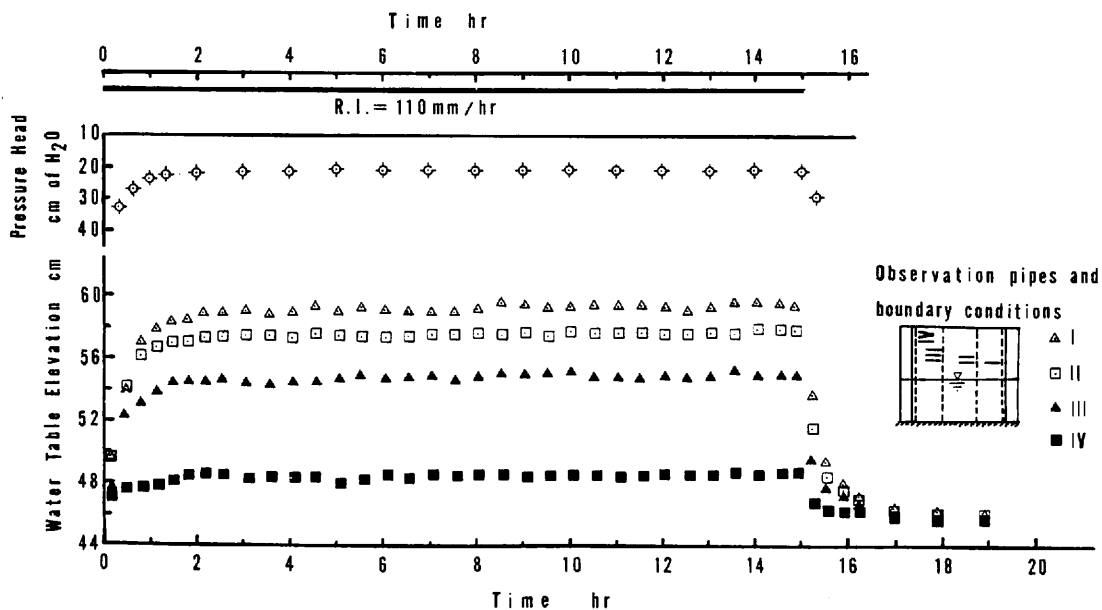


Fig. 4.5 Water table changes during EXP. NO. 9.

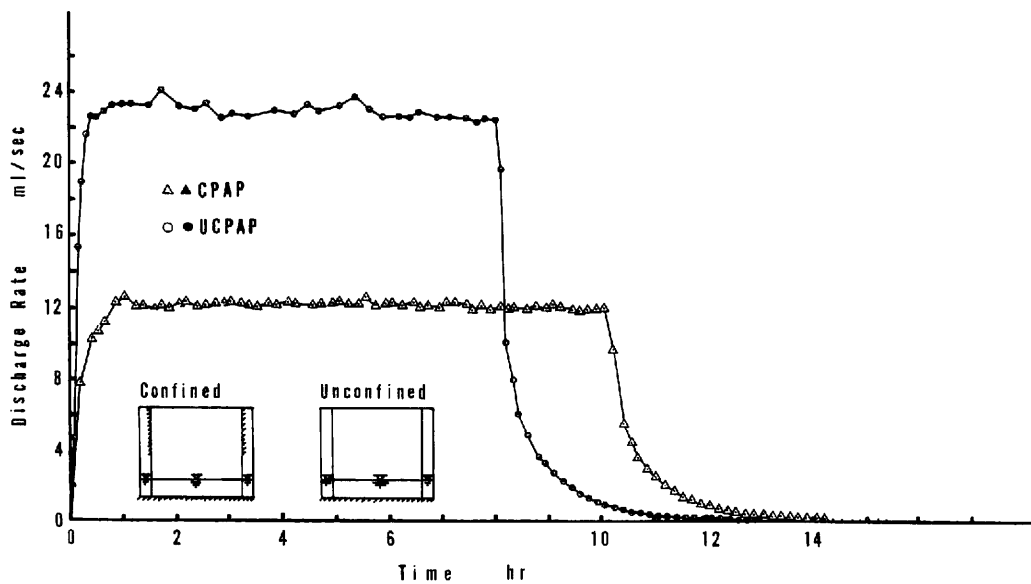
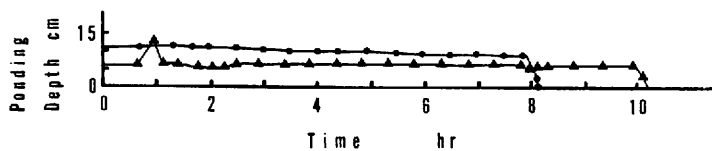


Fig. 4.6 Combination of the discharge hydrographs for EXPS. NO. 11 and 17.

the *UCPAP* experiment was doubled than the *CPAP* ponding experiment, since with the same inflow rate as in the *CPAP* experiment, only 5 mm of ponding depth could take place (*EXP. NO. 16* in Table 2.2).

The main differences in these discharge hydrographs are as follows;

The discharge rate of the *UCPAP* ponding experiment reaches to equilibrium faster than the *CPAP* experiment. But the magnitude of pulsation during this experiment is larger than *CPAP* experiment. Moreover, the number of pulsation in the first case is more than the second one.

The pattern of water table changes during *EXP. NO. 11* is shown in Fig. 4.7. This figure demonstrates that the water table does not fluctuate in response to the ponding infiltration, if the ponding depth remains at a constant level.

From the results of the *CPAP* and *UCPAP* rainfall and ponding infiltration experiments explained above, and consideration in Tables 2.1 and 2.2, the significance of the initial location of capillary zone from the ground surface can be realized clearly.

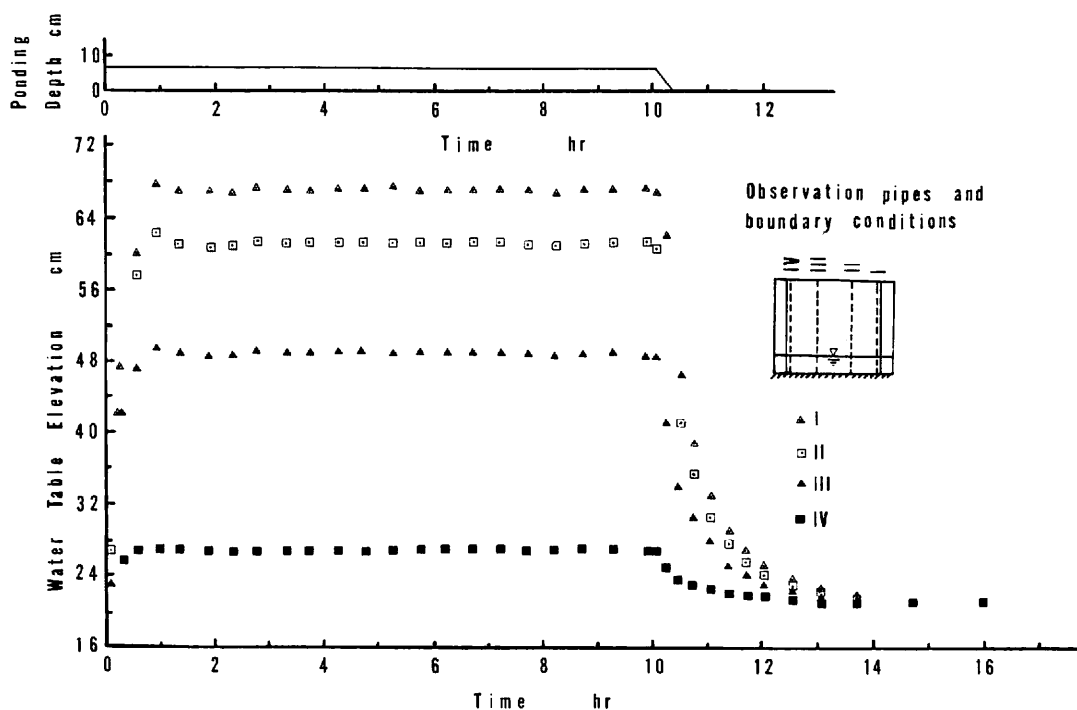


Fig. 4.7 Water table changes during *EXP. NO. 11*.

4.3 The behavior of pressure head in a pulsating flow System

During the experiments discussed in previous section, it was seen that the total potentials of the sand tank simultaneously fluctuated with that of the discharge rate and the water table positions. This evidence was especially significant in the top layer of the sand tank where the soil was not initially saturated with water. To evaluate this behavior, the pressure heads were calculated for 5 cm layer below the sand surface from the measured total potentials by using the following relation;

$$h = H - z - H_w \dots \dots \dots (4.1)$$

where H : total potential [L]
 h : pressure head at the point of measurement [L]
 z : elevation of the point from the reference level,
in this case from the base of the sand tank [L]
 H_w : ponding depth [L]

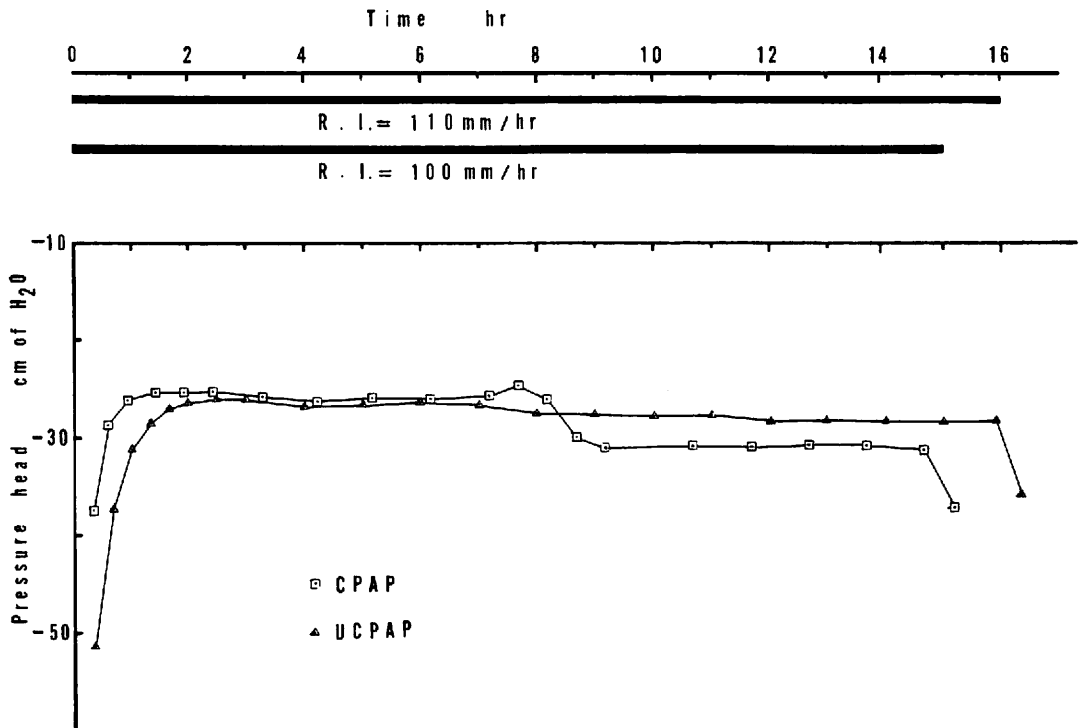


Fig. 4.8 Pressure head variations during EXPS. NO. 4 and 8.

Figure 4.8 shows the pressure head variations during EXPS. NO. 4 and 8. This figure demonstrates that the pressure head for the CPAP experiment is higher at the beginning than the UCPAP experiment. Moreover the pressure head during the CPAP experiment starts to rise with the onset of the rainfall, but it delays in the case of UCPAP one.

During the *CPAP* experiment, the pressure head starts to increase rapidly around 430 minutes and continues until 475 minutes. At this time the pressure head at 5 cm layer below the sand surface reaches to -25 cm of water, but sharply it drops. At 550 minutes of the experiment the pressure head reaches to -30 cm of water. Moreover the pattern of pressure head during the *UCPAP* experiment is smooth from the beginning until the end. There are fluctuations, but very small and almost negligible.

The pressure heads for the *CPAP* and *UCPAP* experiments, (*EXPS. NO. 5* and *9*, respectively) are shown in Fig. 4.9. This figure shows that from the beginning until the end, the pressure head for the *CPAP* experiment is higher than the *UCPAP* experiment's pressure head. In this case it is seen that the *CPAP*'s pressure head fluctuates very irregularly at the beginning, but once it reaches the maximum value, does not change until the end.

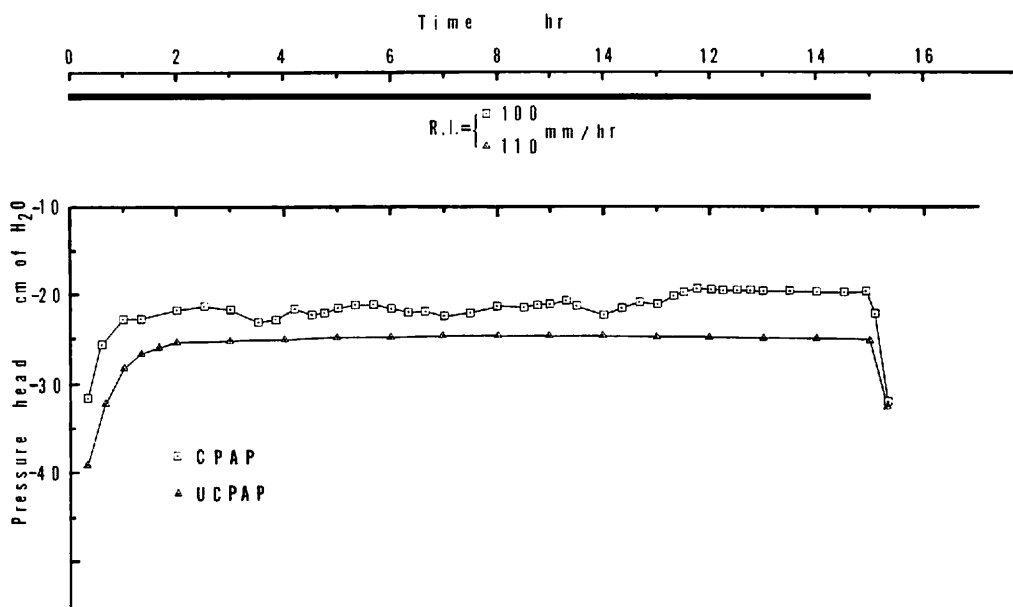


Fig. 4.9 Pressure head variations during *EXPS. NO. 5* and *9*.

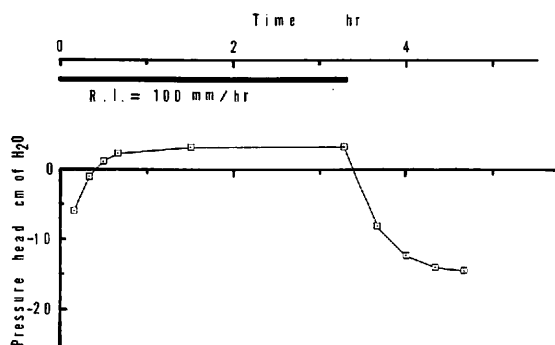


Fig. 4.10 Pressure head variations during *EXP. NO. 6*.

The pressure head values for *EXP. NO. 6* are shown in Fig. 4.10. It was explained in Chapter II, that this experiment was performed when the water table was initially located at 20 cm below the sand surface. In this case as the upper boundary of the saturated capillary zone coincides with the sand surface, after 20 minutes from the start of rainfall, the pressure head of 5 cm layer below the sand surface reached to zero. After this as ponding takes place on the sand surface, the pressure head turns to positive value and continues until the cease of rainfall.

The patterns of pressure head during the *CPAP* and *UCPAP* ponding experiments, i. e., *EXPS. NO. 11* and *17*, respectively, are shown in Figure 4.11. It is seen in this figure that about 6.5 cm of ponded water during *EXP. NO. 11* results the development of positive pressure head after one hour. At the beginning, there are fluctuations in the pressure head, but after 6 hours, it continues at a constant rate.

Although the depth of the ponded water during the *UCPAP* experiment of this series was more than the one during the *CPAP* experiment, it is seen in this figure that the pressure head of the former experiment never reaches to positive value. At the beginning, the pressure head is high, but after 300 minutes it decreases gradually.

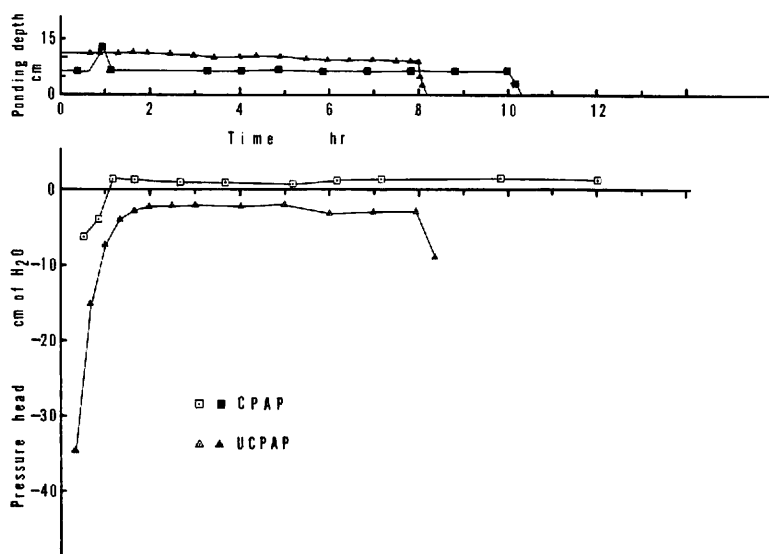


Fig. 4.11 Pressure head variations during *EXPS. NO. 11* and *17*.

To determine the effect of pore-air pressure on the soil profile, the vertical profiles of pressure heads during *EXPS. NO. 4* and *8* are shown in Fig. 4.12a, b, c, d, e and f. It is seen that soon after the start of the ponding, the pressure head near the sand surface moves higher under *CPAP* than the *UCPAP* case. By continuing the infiltration process, the pressure heads near the sand surface become more or less equal, but later the pressure head of the *UCPAP* experiment exceeds the *CPAP*'s one. This difference is especially great in the unsaturated capillary zone. The pressure heads of both experiments between 430 and 490 minutes become equal for some period, but later the *CPAP* experiment's pressure head becomes smaller than the *UCPAP*'s case.

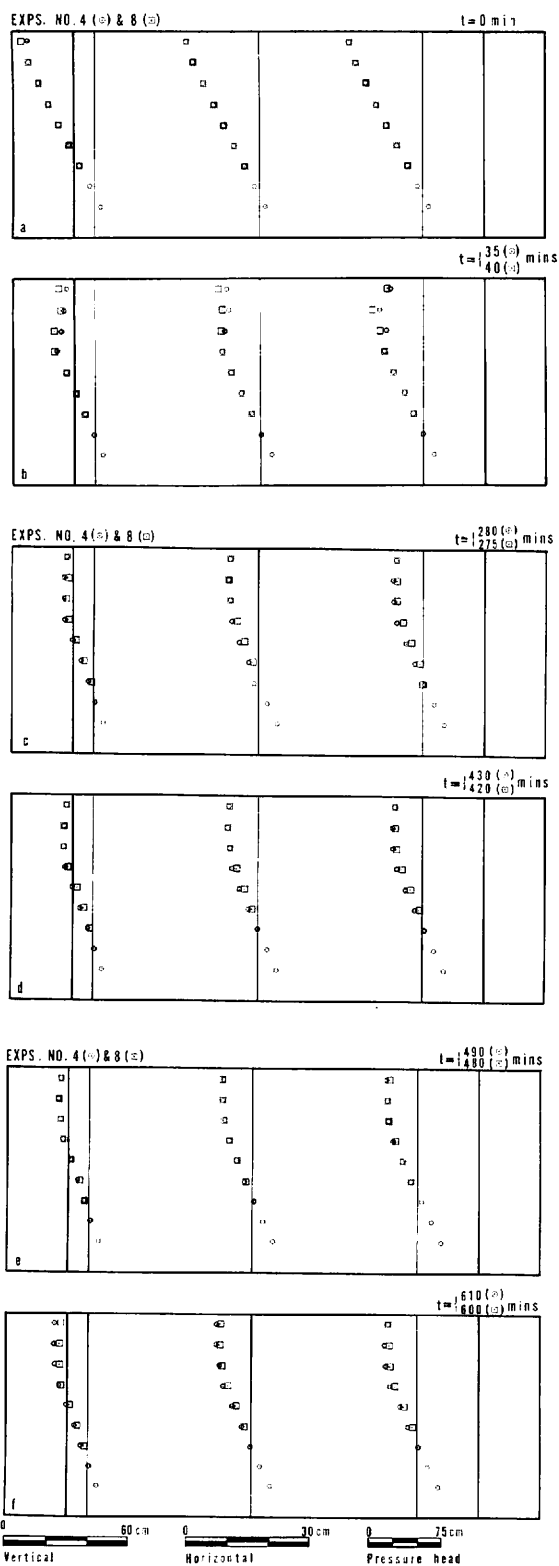


Fig. 4.12 Pressure head profiles for the inlet zone, the middle and the outlet zone of the sand tank during EXPS. NO. 4 and 8.

The pressure head profiles of the ponding experiments namely, *EXPS. NO. 11* and *17* are shown in Fig. 4.13a, b, c and d. It can be seen that at the beginning, the pressure heads above the water table in both of the experiments are negative. But later the pressure heads for the *CPAP* experiment reach to positive value faster than the *UCPAP*'s case. However the pressure head for the *UCPAP* experiment never exceeds the zero value.

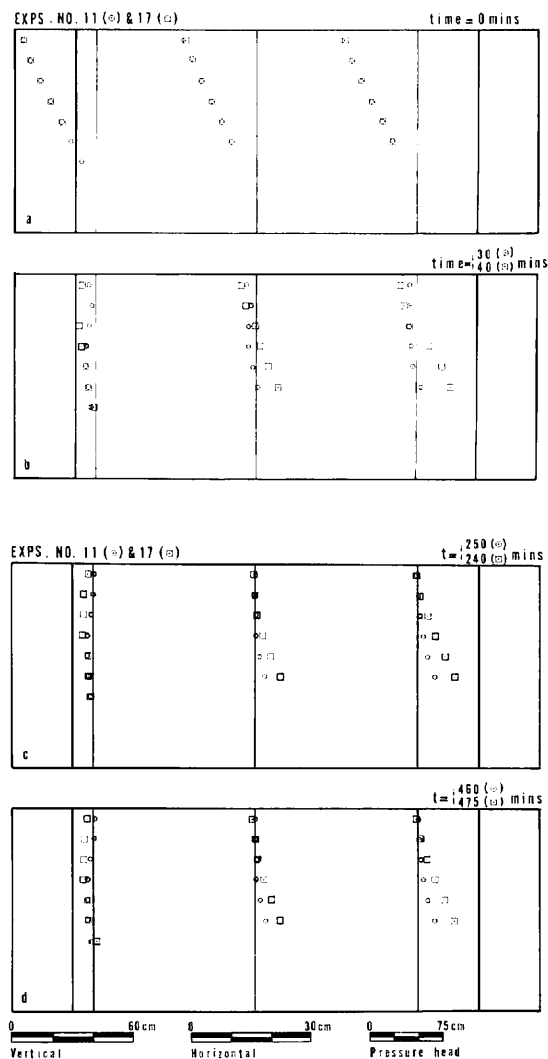


Fig. 4.13 Pressure head profiles for the inlet zone, the middle and the outlet zone of the sand tank during *EXPS. NO. 11* and *17*.

4.4 The behavior of flow in a pulsating flow system

In previous sections it was seen that during the confined pore-air pressure experiments, the discharge rate, the water table positions as well as the pressure heads of the flow system were following unsteady paths. Therefore, it seems necessary to investigate the pulsation concept in the flow pattern of these systems.

The flow patterns of *EXP. NO. 4* at 35 minutes are shown in Fig. 4.14. It is seen in this figure that a zone of uniform hydraulic gradient is developed at the top soil, extending 35 cm below the sand surface. At this time the water table at the inlet boundary rose about 4 cm higher than the initial position, but at the outlet boundary it rose only 2 cm. At the middle part of the sand tank the development of groundwater mound can be visualized. For this reason, the hydraulic condition inside the saturated zone shows the flow of water to both directions, *i. e.*, toward the inlet and the outlet chambers of the sand tank.

When these behaviors are evaluated at 115 minutes of this experiment shown in Fig. 4.15, apparently the zone of uniform hydraulic gradient has not moved further downward. At this time the water table was able to rise 14 cm at the inlet and 4 cm at the outlet boundaries of the sand tank than at 35 minutes position. Due to a high hydraulic gradient, the groundwater mound above the water table has disappeared completely. Likewise it can be seen that the flow is almost vertical until reaching the upper boundary of the saturated capillary zone, but its direction changes toward the outlet boundary as it enters inside the saturated capillary zone. However, water near the inlet boundary of the saturated zone does not show active contribution to the outflow. From these flow patterns it can also be seen that about half of the flow from the sand tank discharges from the vicinity of water level in the outlet chamber.

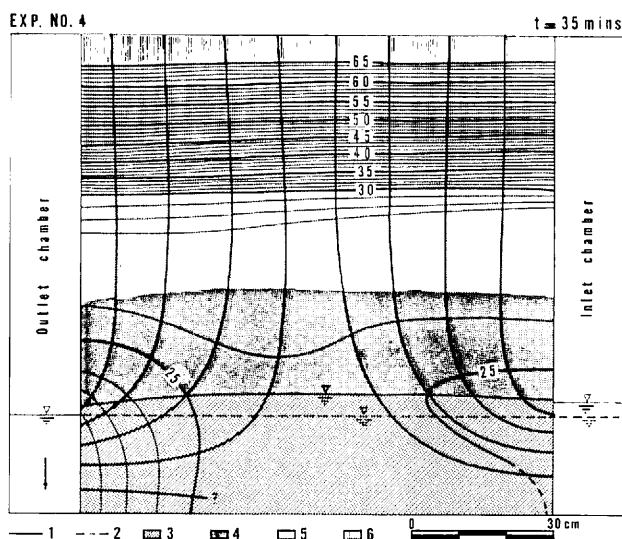


Fig. 4.14 Flow patterns for *EXP. NO. 4* at 35 minutes.

- 1 : Water table position at 35 minutes;
- 2 : Water table position at initial condition;
- 3 : Saturated zone;
- 4 : Saturated capillary zone;
- 5 : Unsaturated capillary zone;
- 6 : Seepage zone.

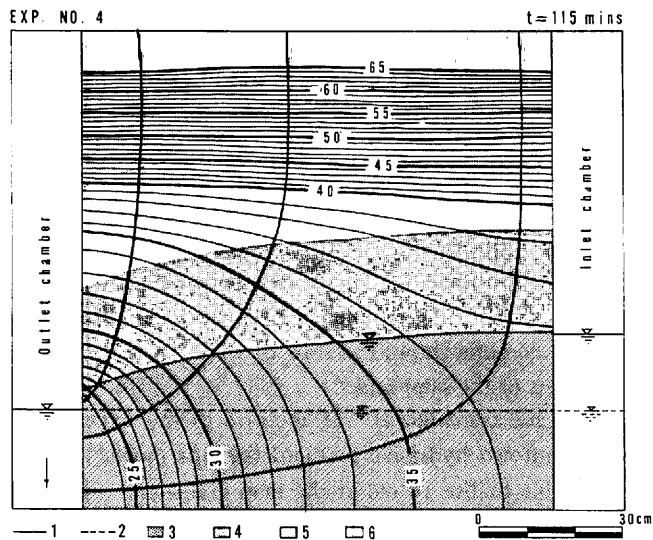


Fig. 4.15 Flow patterns for *EXP. NO. 4* at 115 minutes.

- 1 : Water table position at 115 minutes;
- 2 : Water table position at initial condition;
- 3 : Saturated zone;
- 4 : Saturated capillary zone;
- 5 : Unsaturated capillary zone;
- 6 : Seepage zone.

The flow patterns of the sand tank at 430 minutes of this experiment are illustrated in Fig. 4.16. At this time the discharge rate and the water table are in the rising condition. It is seen that although the position of water table has not changed from the position at 115 minutes, a small increase in the hydraulic gradient has taken place. This is known to be the cause of the increase in the discharge rate.

The flow patterns of the sand tank at 490 minutes is shown in Fig. 4.17. At this time although the discharge rate has started to drop from the maximum value (from 5.2 ml/sec to 4.8 ml/sec), the water table position is about 3 cm higher than it was at 430 minutes. This results about 20% of increase in the hydraulic gradient than before.

Finally the flow patterns at 730 minutes of this experiment shown in Fig. 4.18 depicts the return to normal of the hydraulic condition in the sand tank. At this time the water table has dropped about 3 cm than at 490 minutes.

When the hydraulic conditions of the sand tank at 100 and 390 minutes of *EXP. NO. 8* are considered in Fig. 4.19 and 4.20 respectively, great changes are not observed between these flow patterns. The existence of a small difference in the hydraulic head is because at 100 minutes of the experiment the discharge was not yet reached to a steady condition. The water table rose in the inlet boundary only 3.5 cm at 390 minutes than at 100 minutes. In this case also percolation of water in the unsaturated layer is vertical until reaching the upper boundary of the saturated capillary zone. As they enter in the saturated capillary zone, they change their direction toward the exit boundary.

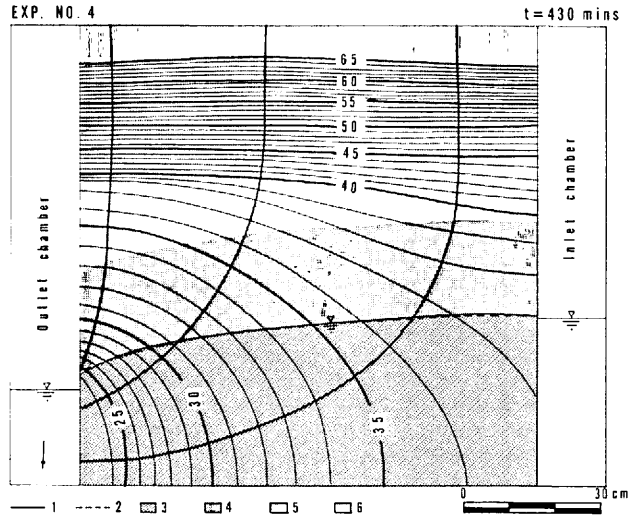


Fig. 4.16 Flow patterns for *EXP. NO. 4* at 430 minutes.

- 1 : Water table position at 430 minutes;
- 2 : Water table position at 115 minutes;
- 3 : Saturated zone;
- 5 : Unsaturated capillary zone;
- 6 : Seepage zone.

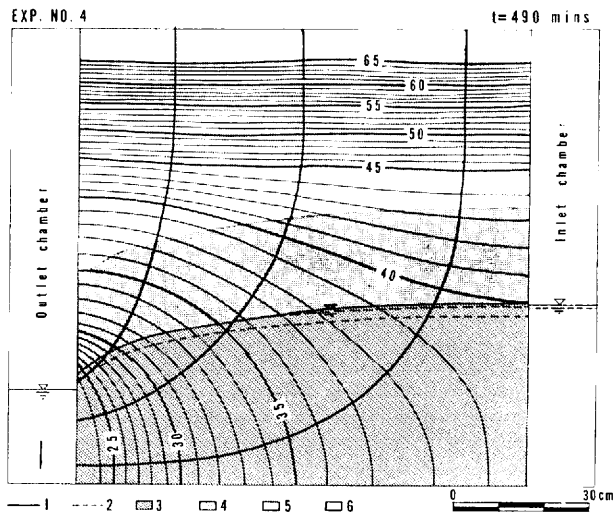


Fig. 4.17 Flow patterns for *EXP. NO. 4* at 490 minutes.

- 1 : Water table position at 490 minutes;
- 2 : Water table position at 430 minutes;
- 3 : Saturated zone;
- 4 : Saturated capillary zone;
- 5 : Unsaturated capillary zone;
- 6 : Seepage zone.

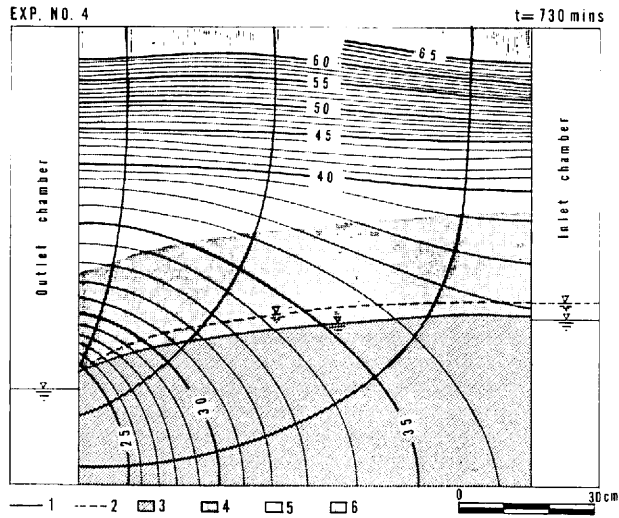


Fig. 4.18 Flow patterns for *EXP. NO. 4* at 730 minutes.

- 1 : Water table position at 730 minutes;
- 2 : Water table position at 490 minutes;
- 3 : Saturated zone;
- 4 : Saturated capillary zone;
- 5 : Unsaturated capillary zone;
- 6 : Seepage zone.

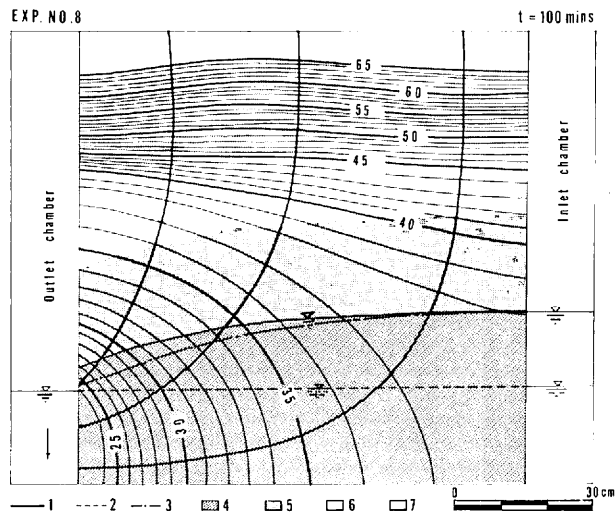


Fig. 4.19 Flow patterns for *EXP. NO. 8* at 100 minutes.

- 1 : Water table position at 100 minutes;
- 2 : Water table position at initial condition;
- 3 : Water table position at 55 minutes;
- 4 : Saturated zone;
- 5 : Saturated capillary zone;
- 6 : Unsaturated capillary zone;
- 7 : Seepage zone.

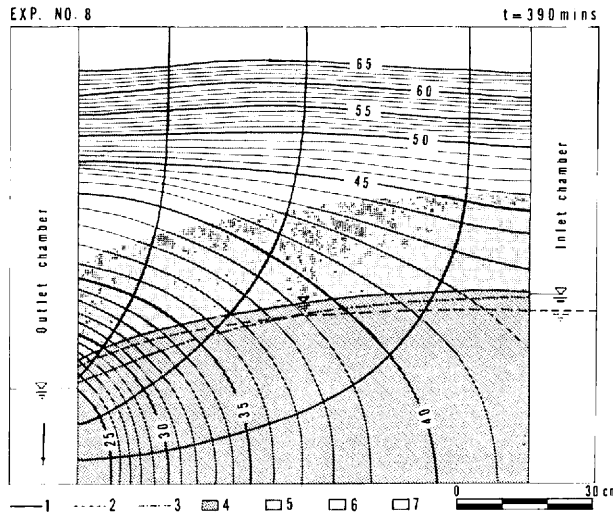


Fig. 4.20 Flow patterns for *EXP. NO. 8* at 390 minutes.

- 1 : Water table position at 390 minutes;
- 2 : Water table position at 240 minutes;
- 3 : Water table position at 100 minutes;
- 4 : Saturated zone;
- 5 : Saturated capillary zone;
- 6 : Unsaturated capillary zone;
- 7 : Seepage zone.

4.5 Quantitative analysis

From the results of *EXP. NO. 4* it was seen that in spite of a constant rainfall application on the sand bed, a considerable pulsation took place at 420 minutes of the experiment. The discharge rate started to increase at this time from an average value of 4.2 ml/sec and reached to 5.2 ml/sec around 475 minutes. Consequently, the discharge after reaching the maximum value dropt back and continued at a lower rate than the average rate before 420 minutes. During this transient period there was an increase of 20% in the discharge rate. The average value of 4.2 ml/sec corresponded to an average value of the rainfall intensity, but 5.2 ml/sec of the discharge rate should be drawn from the water stored before the transient event in the soil pores. It is obvious that extra forces are required to break the equilibrium state of a system.

To deal with this problem, at first the water balance during the experiment was studied. In this laboratory experiment, the evaporation factor was assumed to be negligible. The results of the water balance calculation for *EXP. NO. 4* are shown in Fig. 5.10. It is seen from this figure that the storage of water in the soil pores has taken place for about 115 minutes from the start of the rainfall. After 115 minutes the discharge became equal to the amount of inflow, and continued at this rate until 420 minutes.

To investigate the force that caused the stored water to be discharged from the soil pores, flow net analysis was performed on the potential distributions of the sand tank, using Figs. 4.14, 4.15, 4.17 and 4.18. The calculated discharge rates are compared with the measured values. They show 16% of maximum difference. The results are shown in Table 4.1.

Table 4.1 Quantitative results of the flow net analysis for *EXP. NO. 4*.

Time	Flux in Saturated Zone	Flux in Saturated Capillary Zone	Total Flux	Net Head	Width	Calculated Discharge	Measured Discharge	Difference
min	cm/sec	cm/sec	cm/sec	cm	cm	ml/sec	ml/sec	ml/sec
35	0.017	0.011	0.028	5.8	15	2.436	2.130	0.306
115	0.010	0.006	0.016	15.8	15	3.792	4.189	0.397
430	0.011	0.005	0.016	18.7	15	4.488	4.824	0.336
730	0.009	0.008	0.017	15.7	15	4.004	4.213	0.209

In order to understand the causes of the increase in hydraulic gradient in the sand tank, at first, the pressure heads were calculated from the total head. Calculated pressure heads were then converted into water content using the water characteristic curve shown in Fig. 2.4. The changes in storage at different time intervals were then calculated from these water content values and then compared with the changes in storage obtained from the water balance calculations. It was understood that the changes in storage obtained from the pressure head calculations are more than those from the water balance relation.

The infiltration process is a two-phase flow phenomenon. When the pore-air can not escape from the soil pores, it is compressed downward by the infiltrating water. This pore-air compression affects the hydraulic condition of the system considerably. Therefore, the high hydraulic head that leads to show high changes in the storage was considered to be affected by the pore-air compression. In other words, the hydraulic head was thought to be from the summation of the pressure head and the pneumatic head in the soil profile.

In the second, step an assumed pneumatic head was deducted from the total head, measured during the experiment. Based on these values, the changes in storage were again calculated and compared with that of the water balance method. This trial and error procedure was continued until the changes in storage obtained from the total head agreed with the one from the water balance calculation. The final deducted value from the total head was accounted for the pneumatic pressure head at that time. Moreover, the changes in the pneumatic pressure head between each time interval was the pore-air pressure build-up in the sand tank. The results are shown in Fig. 4.21.

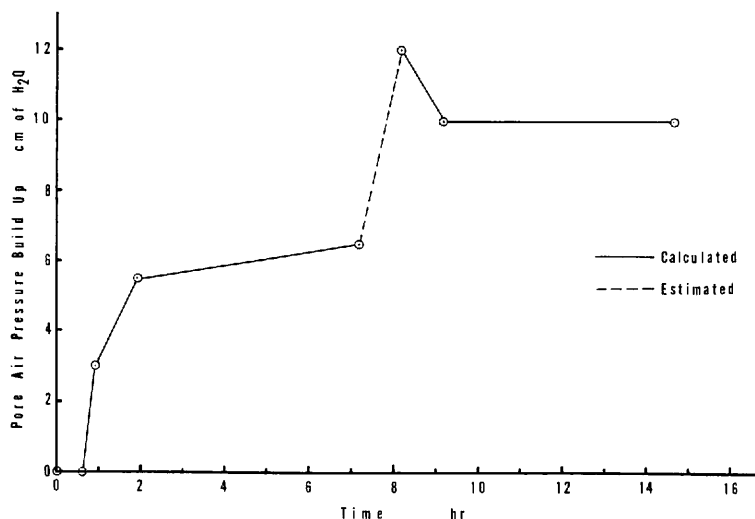


Fig. 4.21 Pore-air pressure build-up during *EXP. NO. 4*.

From this figure it can be seen that the pore-air pressure build-up was slow at the beginning. It started to rise gradually, but after 420 minutes it rose rapidly, reaching the highest value around 475 minutes. Then it dropt. After reaching to 10 cm of H_2O at 550 minutes, thereafter the pressure head continued without changes. This figure reveals that the released pore-air pressure from the soil profile is only an equivalent value to 2 cm of water. The maximum pore-air pressure build-up at 490 minutes is about 12 cm of water. Since the hydraulic head was not recorded just before the air escape, the actual pore-air pressure build-up can be more than the calculated one. For this reason, the pore-air pressure build-up between 430 and 490 minutes are shown by a dashed line. This fact will be delt in detail in the next section.

4.6 Discussion

From the results presented above, it is clear that the occurrence of pulsation in subsurface hydrological phenomena is related to many physical and hydrological factors prevailing in the site. The hydrological factors analyzed in this research generally revealed the importance of the rainfall intensity and its duration. It was also understood that the location of water table from the ground surface has great importances in subsurface flow studies. Because it determines the location of the upper boundary of capillary zone from the ground surface in a flow system.

A comparison of the discharge hydrographs, the water table position as well as the pressure head changes during the *CPAP* and *UCPAP* experiments revealed the fact that the entrapped pore-air in the soil pores has significant impacts on the subsurface hydrological aspects. It was also observed that when the compressed pore-air is not free to escape, it is compressed downward and accumulates into the pores in the lower layers of the soil profile. On the other hand, the upper quasi-saturated layer at the soil surface prevents the air to escape from the soil pores. As a result, the pressure head below the wetting front increases. This fact has been reported by many researchers (e. g., Bouwer, 1969; Vachaud *et al.* 1974).

This phenomenon was clearly observed in *EXP. NO. 4*. Because of an increase in pore-air pressure, the discharge rate and the water table position increased temporarily. But when the same experiment is carried under a small rainfall intensity (*EXP. NO. 2* in Table 2.1), or with the unconfined boundaries, (*EXP. NO. 8* in Table 2.1), this transient behavior was not observed.

From a consideration of the discharge rate, and the pressure head patterns of *EXP. NO. 4*, it is well understood that the air pressure build-up has taken place above the saturated capillary zone and has continued for 420 minutes. This means that 420 minutes was required for the displaced air to become continuous from the dispersed condition.

The results of the pore-air pressure build-up calculations showed that after 430 minutes the pore air pressure increased rapidly from 6.5 cm and reached to 12 cm of water at 490 minutes. At this time the potential at the soil surface has reached to an average value of 70 cm of water. Since this potential is consisting of both the hydraulic and the pneumatic heads, to obtain the net hydraulic head, the contribution of pore-air pressure was deducted. By this method the net pressure head reached to -37 cm of water, which is equivalent to the air entry value of the standard sand used.

The equilibrium water saturation condition of the soil establishes with a pressure head equivalent to the air entry value of that soil. When the developed pore-air pressure becomes larger than the air entry value, the accumulated air breaks the equilibrium condition and escapes from the weak point of the soil profile to the atmosphere. After the escape of air, the soil profile no longer behaves as a confined one. Consequently, it can be thought that the pneumatic pressure head of the accumulated displaced-air has reached near the air entry value of the standard sand before to be released during the experiment from the sand tank.

The water table position changes also revealed an unsteady behavior during the transient period of discharge. As Freeze and Cherry (1979, p. 232) reported the abnormal rise in the water levels in the observation wells during heavy rainstorms have been observed in shallow unconfined aquifers. In the case of *EXP. NO. 4*, the rise of water table position in the sand tank during this transient period reached to 3 cm at the time of measurement. The fact that the water table is the lower boundary of the saturated capillary zone brings one to realize that the rise of water table within this zone indicates only the changes of pressure head to the positive value. Therefore, the developed 12 cm of water of pore-air pressure build-up in the upper layers of capillary zone caused the pressure head of 3 cm of the saturated capillary zone to become positive.

When the discharge hydrograph of this experiment is compared with that of the *EXP. NO. 8*, the discharge hydrograph of *EXP. NO. 8* also reveals a discontinuity in the discharge rate around 430 minutes. This indicates that even in the case of unconfined boundaries, the pore-air pressure build-up takes place. Since the air can escape laterally from the soil pores, it does not build up to the limit to bring the pore-air pressure near the air entry value. Consequently no considerable pulsation took place during *EXP. NO. 8*.

When the water table in a soil profile reaches to a position that the upper boundary of capillary zone coincides with the ground surface, the chance of air-water interchange becomes great. Since under such conditions the depth of quasi-saturated zone at the soil surface is not great, the air can escape from the soil pores frequently. If air can not escape laterally, it builds up, but can not reach the air entry value of the soil material. Therefore, the pulsations that take place under such conditions have small magnitudes. It was seen in Figs. 4.4 and 4.9 that the discharge rate and the pressure head continued with small fluctuation for long time. It can be seen in the

discharge hydrograph that the discharge rate is less than the average amount of rainfall for about 12 hours. Consequently, it is thought that the air-water interchange in the soil profile prevents the hydraulic gradient to rise. From the pattern of the discharge fluctuation it was also understood that the displacement of air from the soil pores is accomplished gradually, because the decrease in the magnitude of these fluctuations are gradual (Fig. 4.4). After about 12 hours when the continuity of air from the soil profile is demolished, the hydraulic gradient starts to rise. As a result, the discharge rate reaches equal to the inflow rate and the pressure head also becomes stable.

During the ponding experiments, namely *EXP. NO. 11* and *17*, the discharge started within less than a minute after the application of ponding. Nevertheless, in the case of *UCPAP* experiment, the discharge started after 2.75 minutes, but reached to the maximum value without delay. Some pulsations certainly took place, but they are not accounted due to the entrapped pore-air, since no air escape was observed through the sand surface.

It can be concluded that the existence of pore-air in any condition, namely in the entrapped, or the displaced form, affects the subsurface hydrological character of a soil profile, and results transient impacts on that system. This effect is especially great in places where the water table lies some distance from the ground surface. Moreover the significance of the type of infiltration, *i. e.*, rainfall or ponding, are also very distinctive.

Consequently, the condition of pore-air in a soil profile strongly affects the hydraulic gradient and causes the system to act as an unsteady one. For this reason Brustkern and Morel-Seytoux (1970) recognized the effect of pore-air and recommended that for a physically realistic treatment of infiltration problem, the air-phase must be given full consideration.

CHAPTER V

FLOW BEHAVIOR IN THE VICINITY OF SEEPAGE FACE

5.1 General aspects

The horizontal flow line assumption of the Dupuit-Forchheimer's theory discussed in Chapter III neglects the vertical flow existing in a system. This infirmity of the theory leads an incorrect configuration of the shape of water table in the soil profile. As a result, a seepage face can not be developed at the exit face of a flow system by using the Dupuit-Forchheimer's theory. Among others, McWhorter and Sunada (1977, p. 148) discussed this subject in detail. In addition, according to Verruijt (1970, p. 122), due to the non-zero component of the specific discharge vector perpendicular to the boundary, a seepage face is not a streamline for groundwater movement.

The term *seepage face* is interchanged in literature by the "*seepage surface*", "*surface of seepage*" and the "*leakage zone*".

In this Chapter, the condition of flow in the vicinity of seepage face is investigated by examining the hydraulic condition of the sand tank under various experimental conditions. It is also considered to emphasize the influences of entrapped pore-air on the hydraulic condition of the seepage face in a flow system.

5.2 The behavior of flow at the open face of the capillary zone

The open face of the capillary zone to the atmosphere in a watershed carries significant importance with regard to the surface and subsurface flow phenomena. In this section it will be examined to disclose the behavior of this portion of the soil in response to the rainfall and ponding infiltration events.

5.2.1 Due to the rainfall infiltration

It was reported in Section 4.4 that during a rainfall event, the pore-air pressure build-up affects severely the discharge rate and the water table position in a soil profile. This effect is especially great in the flow systems with confined boundary conditions.

The flow patterns of the *CPAP* and *UCPAP* rainfall infiltration experiments (*EXPS. NO. 4* and *8*), discussed in Chapter IV, demonstrated that the seepage face developed during the *UCPAP* experiment (*EXP. NO. 8*) was greater than the one under the *CPAP* experiment (*EXP. NO. 4*). Moreover, the hydraulic gradient at the exit face was the same between 15 and 50 cm from the sand surface during the *EXP. NO. 8*, but it was different in the case of *EXP. NO. 4*. It was also observed that about half of the water reaching the exit face discharged from the neighborhood of the water level in the outlet chamber. Consequently, it can be argued that the entrapped pore-air influences considerably the hydraulic condition of a flow system, including the open face of the capillary zone.

5.2.2 Due to the ponding infiltration

To investigate the flow behavior during the ponding experiment at the open face of the capillary zone, the flow patterns of the *CPAP* and *UCPAP* experiments (*EXPS. NO. 11* and *17* respectively), are discussed in this section.

The flow patterns of *EXP. NO. 11* at 30 minutes are shown in Fig. 5.1. In this figure the atmospheric surface line showing the theoretical position of the water table is also shown. But, actually the water table position was measured at some distance below the sand surface, higher than the piezometric surface. At this time the water level in the inlet chamber rose to 60 cm from the base and 5 cm of the seepage face was developed at the exit boundary of the sand tank.

The flow patterns of the sand tank at 100 minutes of this experiment shown in Fig. 5.2 reveal an increase in hydraulic gradient in all part of the sand tank. At this time flow takes place from a larger portion of the exist face than as it was observed at 30 minutes. From these flow patterns and the pressure head profiles of this experiment shown in Fig. 4.13, it can be realized that at this time a zone of quasi-saturation is developed in the upper layers of the sand tank. Moreover it is seen that more than half of the total flow discharges from the vicinity of water level in the outlet chamber.

In this figure, the location of atmospheric surface line showing the theoretical position of the water table does not coincide with the observed water table position. According to this figure, about half of the sand tank near the inlet boundary from the sand surface to the base is quasi-saturated. But from the middle to the outlet boundary of the sand tank, except a small layer near the sand surface, a zone of unsaturation exists. The thickness of this unsaturated zone becomes larger as it comes closer to the outlet boundary. Conversely, at the exit face the atmospheric surface line lies lower than the observed water table position. This occurs due to the existence of strong vertical component of the flow near the exit face.

The flow patterns of this experiment at 460 minutes are shown in Fig. 5.3. At this time also the above mentioned quasi-saturated zone is existing at the top layers and extends to the water

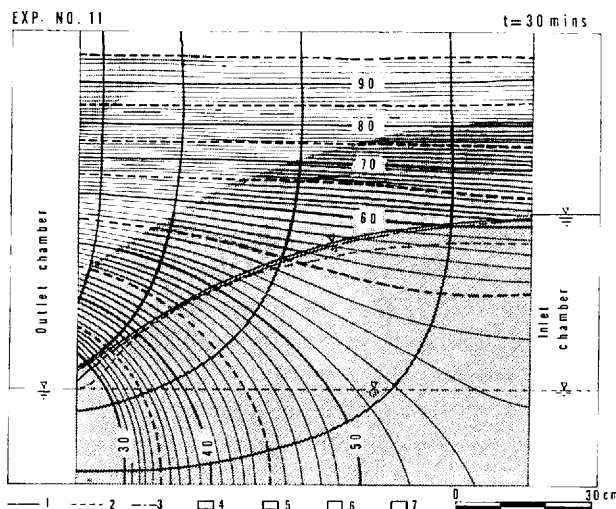


Fig. 5.1 Flow patterns for *EXP. NO. 11* at 30 minutes.

- 1 : Measured water table position;
- 2 : Atmospheric pressure surface;
- 3 : Piezometric surface;
- 4 : Saturated zone;
- 5 : Saturated capillary zone;
- 6 : Unsaturated capillary zone;
- 7 : Unsaturated zone.

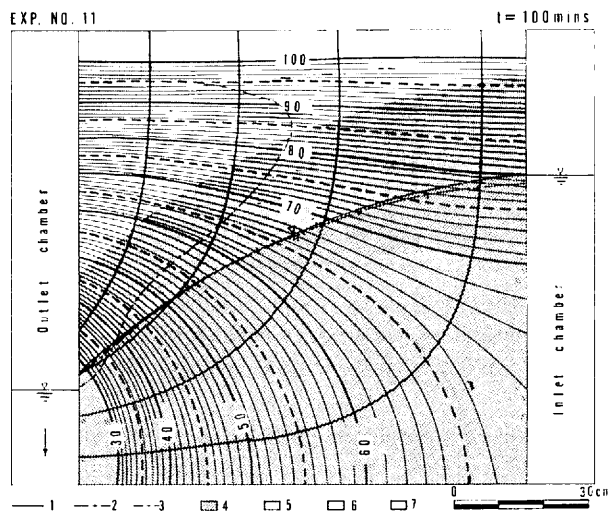


Fig. 5.2 Flow patterns for *EXP. NO. 11* at 100 minutes.

- 1 : Measured water table position;
- 2 : Piezometric surface;
- 3 : Atmospheric pressure surface;
- 4 : Saturated zone;
- 5 : Saturated capillary zone;
- 6 : Unsaturated capillary zone;
- 7 : Unsaturated zone.

table near the inlet zone of the sand tank. Since no great changes are observed in these flow patterns to be due to the entrapped pore-air, it can be argued therefore, that during the ponding infiltration process, the entrapped pore-air escapes from the soil profile at the early stages of infiltration process. Thereafter the air remained in the soil pores is in a dispersed condition and therefore, can not become continuous because of the development of quasi-saturation near the soil surface.

The hydraulic condition of the sand tank at 40 minutes of *EXP. NO. 17* is shown in Fig. 5.4. In contrast to the results of *EXP. NO. 11*, in this case a horizontal flow is developed in the saturated zone. But in the upper parts of the sand tank the flow is lateral. Although this figure indicates the existence of the flow from the open face of the capillary zone, the existence of negative pressure head makes this possibility doubtful.

The hydraulic condition of the sand tank at 100 minutes of *EXP. NO. 17* is shown in Fig. 5.5. At this time the existence of lower piezometric surface than the atmospheric one indicates the presence of downward water movement. The hydraulic gradient at the exit face within the capillary zone has not changed significantly, but great changes were noticed in the upper layers than as observed at 40 minutes. In contrast with the *CPAP* experiment, at this time the whole zone above the atmospheric surface in the sand tank was in quasi-saturated condition.

There are small changes in the hydraulic condition of this experiment at 240 minutes shown in Fig. 5.6 than at 100 minutes. The location of the atmospheric and the piezometric surfaces as well as the hydraulic gradient have not changed significantly at the exit face. This indicates that the hydraulic condition of the sand tank is reaching to a steady state.

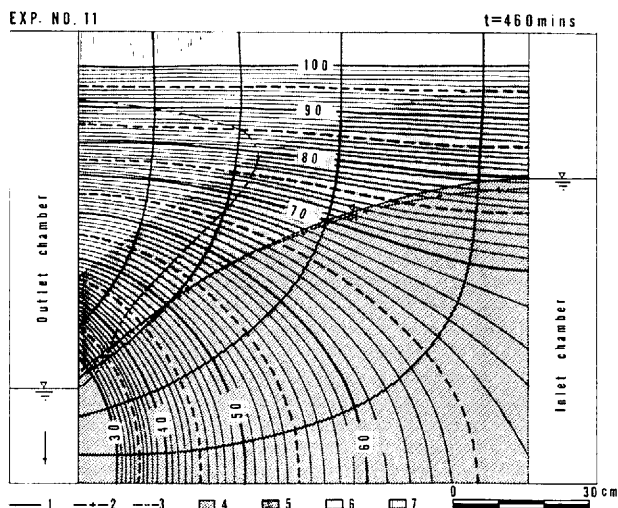


Fig. 5.3 Flow patterns for *EXP. NO. 11* at 460 minutes;

- 1 : Measured water table position;
- 2 : Piezometric surface;
- 3 : Atmospheric pressure surface;
- 4 : Saturated zone;
- 5 : Saturated capillary zone;
- 6 : Unsaturated capillary zone;
- 7 : Unsaturated zone.

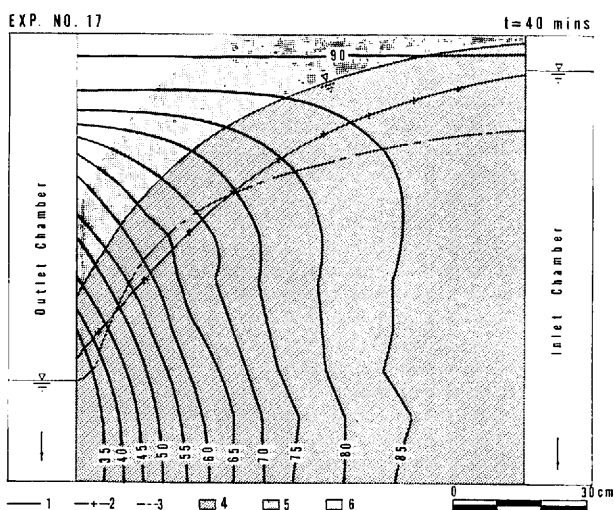


Fig. 5.4 Hydraulic condition of the sand tank at 40 minutes of *EXP. NO. 17*.

- 1 : Measured water table position;
- 2 : Piezometric surface;
- 3 : Atmospheric pressure surface;
- 4 : Saturated zone;
- 5 : Saturated capillary zone;
- 6 : Unsaturated capillary zone.

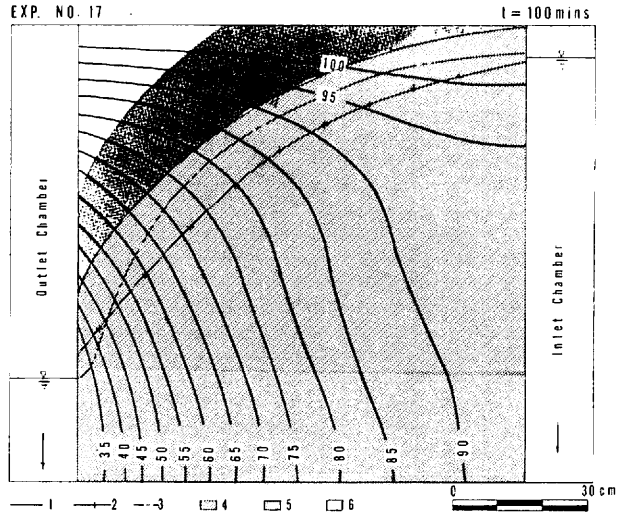


Fig. 5.5 Hydraulic condition of the sand tank at 100 minutes of *EXP. NO. 17*.

- 1 : Measured water table position;
- 2 : Piezometric surface;
- 3 : Atmospheric pressure surface;
- 4 : Saturated zone;
- 5 : Saturated capillary zone;
- 6 : Unsaturated capillary zone.

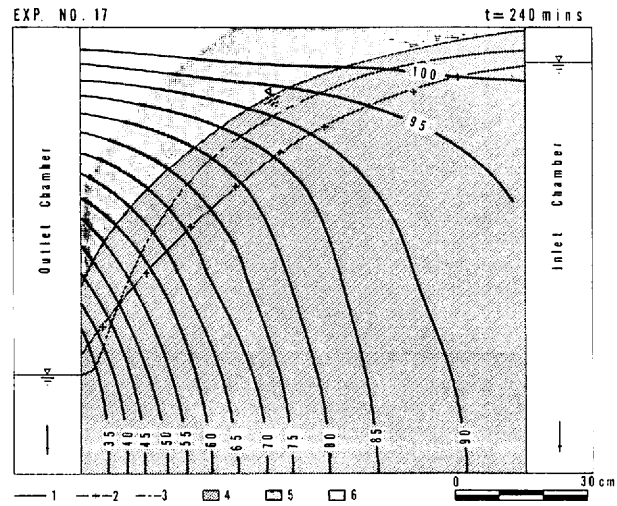


Fig. 5.6 Hydraulic condition of the sand tank at 240 minutes of *EXP. NO. 17*.

- 1 : Measured water table position;
- 2 : Piezometric surface;
- 3 : Atmospheric pressure surface;
- 4 : Saturated zone;
- 5 : Saturated capillary zone;
- 6 : Unsaturated capillary zone.

5.3 Characteristics of flow in the seepage face

The characteristics of flow in the seepage face is studied in this section under the rainfall and ponding infiltration experiments. For this purpose, to quantify the amount of water being discharged from here, the flow channel reaching from the soil surface to the seepage face was separated in each flow diagram. The shapes of the flow lines in each case can depict the flux angle in the vicinity of seepage face graphically. The flow diagrams for *EXPS. NO. 4, 8* and *11* are shown in Figs. 5.7, 5.8 and 5.9., respectively.

5.3.1 Due to the rainfall infiltration

The flow patterns of *EXP. NO. 4* at 35 minutes shown in Fig. 4.14 demonstrated that only 2 cm of seepage face was developed at that time. From the evaluation of the flow diagram of this experiment in Fig. 5.7 it is understood that 5% of the flow at the sand surface is discharged from the seepage face. Moreover, the condition of the flow lines here also shows that the flow is accompanied with horizontal and vertical components.

As the infiltration process continues, at 115 minutes (Fig. 4.15) the seepage face expands upward to 4.2 cm and its contribution to the discharge evaluated from Fig. 5.7, reaches to 9%, of the total inflow. At 430 minutes of this experiment as shown in Fig. 4.16, although the length of the seepage face did not change, but 12.2% of water was discharged from here.

When the behavior of flow at the seepage face is evaluated for 100 minutes of *EXP. NO. 8*, (Fig. 4.19), it can be understood that 6.2 cm of seepage face has been developed at this time. At 390 minutes (Fig. 4.20) of this experiment the length of seepage face did not change. Furthermore, when the condition of flux at the seepage face at this time is evaluated from Fig. 5.8, only small changes in the condition of flux at this time can be observed than at 100 minutes.

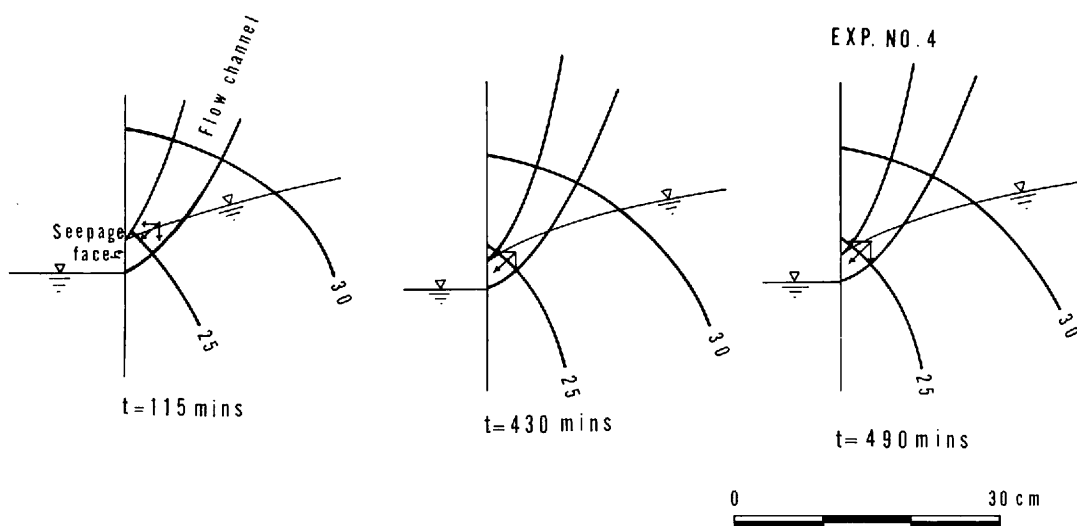


Fig. 5.7 Flow diagram of the seepage face during *EXP. NO. 4*.

5.3.2 Due to the ponding infiltration

The flow patterns at 30 minutes of *EXP. NO. 11* presented in Fig. 5.1 show the development of only 1.5 cm of seepage face. The vertical hydraulic gradient in the seepage face does not show greater difference compared with that of the open face of the capillary zone. The condition of flow discharged from the seepage face is shown in Fig. 5.9. This figure demonstrates 8% of the discharge from the seepage face.

The flow patterns at 100 minutes of this experiment shown in Fig. 5.2 reveal the expansion of seepage face to 4.2 cm, but only small changes in the hydraulic gradient can be observed in Fig. 5.9. Form this figure it is understood that the amount of discharge coming out of the seepage face reaches to 10.4% of the total inflow.

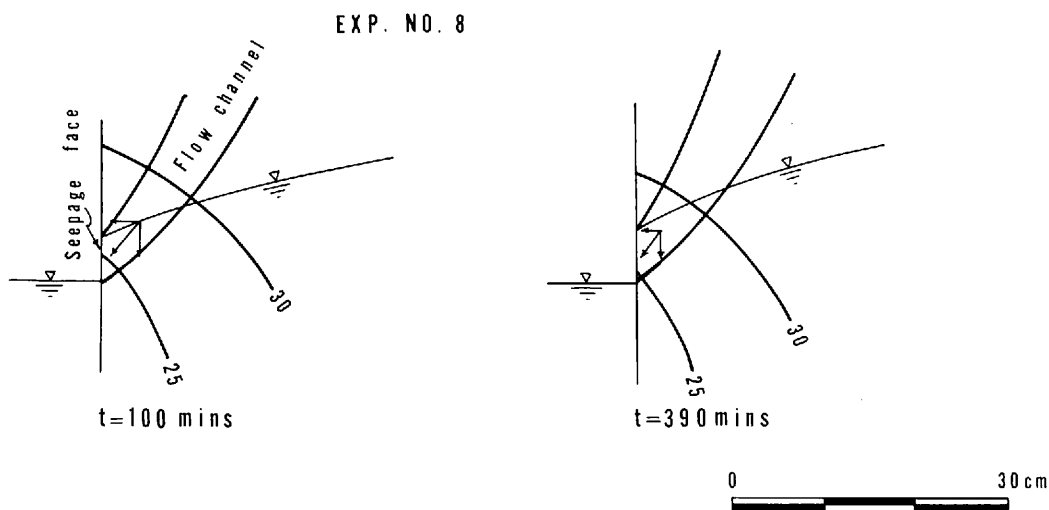


Fig. 5.8 Flow diagram of the seepage face during *EXP. NO. 8*.

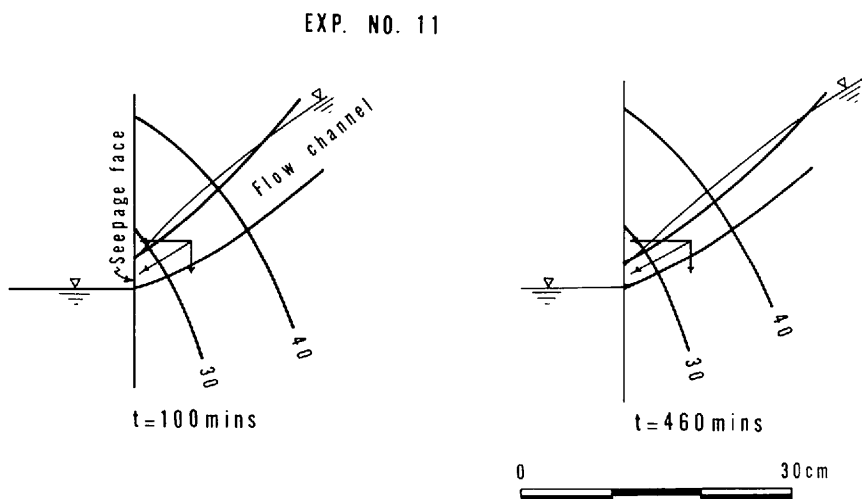


Fig. 5.9 Flow diagram of the seepage face during *EXP. NO. 11*.

The flow condition at the seepage face of this experiment at 460 minutes is shown in Fig. 5.3. This figure reveals a reduction in the length of seepage face, comparing to the one observed at 100 minutes. The vertical hydraulic gradient and the flow components however do not reveal major changes.

When the condition of flow during the *UCPAP* ponding experiment (*EXP. NO. 17*) is considered in Figs. 5.4, 5.5 and 5.6, the line showing the measured water table, indicates the presence of 19 cm of seepage face. In fact water was flowing out of the higher places than 19 cm above the water level in the outlet chamber. During these experiments, the seepage face once developed at the beginning, was observed until the end without significant changes.

5.4 Quantitative analysis

The explanations in the two previous sections on the behavior of flow in the vicinity of seepage face and the open face of the capillary zone require a quantitative analysis of the flux. The results of the flow net analysis performed on the potential distribution of the sand tank for *EXP. NO. 4*, were discussed in Chapter IV. In this chapter the flow net analysis for *EXPS. NO. 8* and *11* was accomplished by using Figs. 4.19, 4.20, 5.1, 5.2 and 5.3. The results of the analysis given in Tables 5.1 and 5.2, were further compared with the measured discharge rates of each experiment. They show good agreements with the observed values.

Table 5.1 Quantitative results of the flow net analysis for *EXP. NO. 8*

Time	Flux in Saturated Zone	Flux in Saturated Capillary Zone	Total Flux	Net Head	Width	Calculated Discharge	Measured Discharge	Difference
min	cm/sec	cm/sec	cm/sec	cm	cm	ml/sec	ml/sec	ml/sec
100	0.010	0.007	0.017	17.4	15	4.437	4.300	0.137
390	0.010	0.005	0.015	20.5	15	4.612	4.740	0.128

Table 5.2 Quantitative results of the flow net analysis for *EXP. NO. 11*

Time	Flux in Saturated Zone	Flux in Saturated Capillary Zone	Total Flux	Net Head	Width	Calculated Discharge	Measured Discharge	Difference
min	cm/sec	cm/sec	cm/sec	cm	cm	ml/sec	ml/sec	ml/sec
30	0.011	0.006	0.017	47	15	11.985	10.750	1.235
100	0.010	0.005	0.015	52.9	15	11.902	12.100	0.198
460	0.010	0.005	0.015	53.3	15	11.992	12.230	0.238

It is seen that the results of the flow net analysis of *EXP. NO. 4* indicate major differences with the measured values comparing with the other experiments. As discussed earlier, this is because of a high pore-air pressure build-up during this experiment. To compare these results with the water balance calculations, the schematic representation of the water balance calculations are given in Figs. 5.10, 5.11, 5.12 and 5.13 for *EXPS. NO. 4, 8, 11* and *17*, respectively. The effects of pore-air on the water balance of the flow system can be disclosed by comparing the changes in the storage of *CPAP* experiments with that of the *UCPAP* ones. This effect is significant especially in the case of rainfall infiltration experiments.

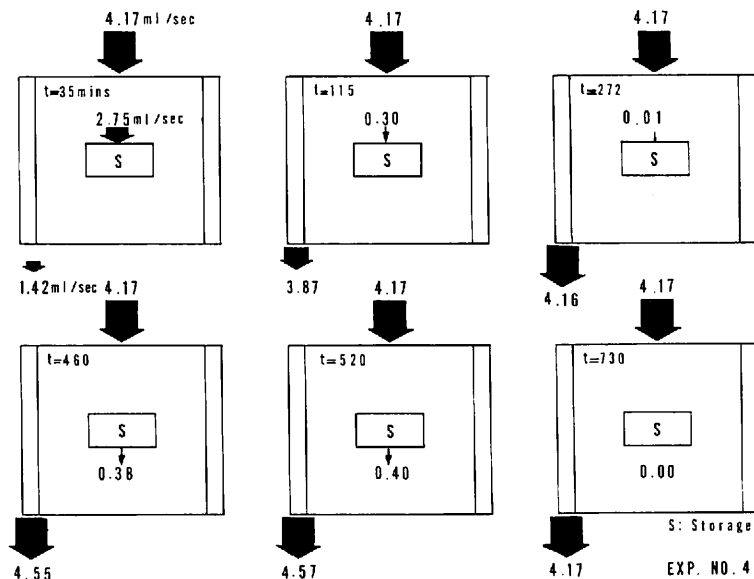


Fig. 5.10 Schematic representation of the water balance for *EXP. NO. 4*.

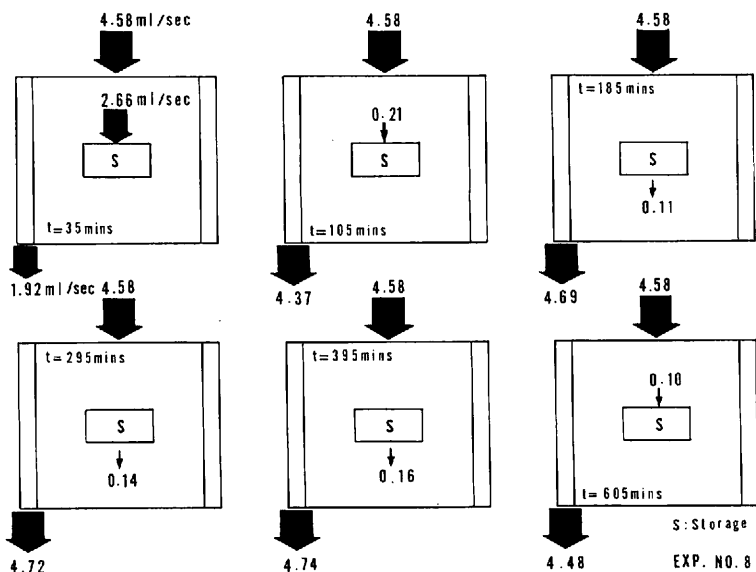
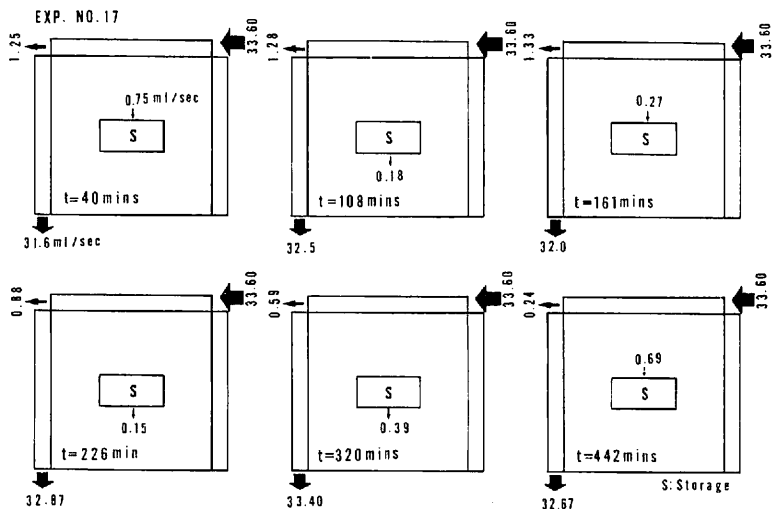
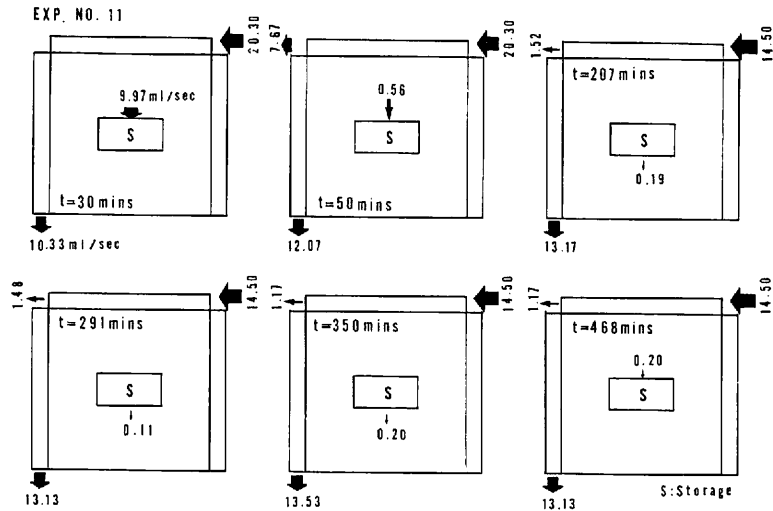


Fig. 5.11 Schematic representation of the water balance for *EXP. NO. 8*.



The flow diagrams of the seepage face under different experimental condition showed that the size of the flow channel at the sand surface reaching to the seepage face did not exceed 12% of the total length of the sand tank. But from the observed hydraulic gradient at the exit face during the ponding experiment, more than 12% of the total inflow was anticipated to be discharged from the seepage face. This hydraulic gradient is thought to be affected by the entrapped pore-air at this face as discussed in Chapter IV.

5.5 Discussion

By examining the hydraulic and hydrological parameters of the experiments in Chapter IV, the role of entrapped pore-air in relation to subsurface flow was made clear. This subject was further examined by using the hydraulic parameters to estimate the amount of entrapped pore-air pressure build-up causing the transient behavior in the system. In this chapter it is seen that the combination of pore-air effect and probably the existence of throughflow through the macropores of the soil profile causes the hydraulic gradient to become large at the exit face of a system.

An evaluation of the shape of potential lines at the exit face during the rainfall as well as in the ponding infiltration experiments indicate the existence of large vertical component of the flow at the seepage face. Moreover, these results likewise revealed the non-existence of a horizontal flowline network. Hence the horizontal flow line assumption of the D-F's theory seems to be invalid. Secondly the condition of flux at the vicinity of seepage face was discussed. From the analysis of flow lines at the seepage face during the *CPAP* and *UCPAP* of the rainfall and ponding experiments, it is observed that the hydraulic gradient near the exit face obtains high values, probably more than one.

Basically the Darcy's law is written in the following form:

$$Q = i \cdot K_s \cdot A \dots\dots\dots (5.1)$$

- where Q : the amount of discharge [$L^3 T^{-1}$]
 i : hydraulic gradient [L/L]
 A : cross sectional area [L^2]
 K_s : saturated hydraulic conductivity [LT^{-1}]

Among these parameters, the only one capable of large extent of variation is the hydraulic gradient. This can be influenced by the depth of ponding and also by the pore-air pressure. The maximum value of the hydraulic gradient in a system does not exceed the unity unless the effect of pore-air and the ponding depth affect the flow behavior. It was seen that during the rainfall infiltration experiment, the increase of pore-air pressure caused the discharge rate, the water table position and the pressure head of the soil profile to increase temporarily. But during a ponding infiltration experiment, because of the effects of the ponded water and of the pore-air, the hydraulic gradient can be thought to exceed the unity.

CHAPTER VI

DISCUSSION

6.1 Mechanism of pulsation in subsurface flow systems

It was mentioned earlier that the occurrence of pulsation in subsurface hydrological phenomena results because of the existence of soil piping, the presence of small hydraulic gradient, hysteresis (ink-bottle and the rain drop effects, Bear, 1979, p. 200) and because of the entrapped pore-air effects. It should be noticed that each of these concepts carry different mechanism. In this study however, the pulsation concept is studied with the effects of entrapped pore-air.

The existence of the capillary zone close to the ground surface causes the pressure head at the top soil to be large. Under such conditions, the soil pores are filled with water in short duration. When the infiltrating water crosses the soil-air interface, the smallest pores of the soil profile are filled with water at first. Thereafter the displaced air from smaller pores try to escape upward if the conditions of the neighbouring pores are favorable. In the other case, they are compressed downward into the soil pores. By the establishment of a wetting front near the soil surface, the upward movement of air at lower layers is further restricted. Therefore, they remain among the larger pores. The downward advance of the wetting front reduces gradually the void space and compresses the entrapped pore-air further downward. This process continues until the entrapped-air in the soil pores below the wetting front makes a body of air. At this time the partial pressure of the accumulated air is greater than its initial partial pressure in the dispersed condition. The increase of the partial pressure of the accumulated pore-air follows the ideal gas law.

The accumulation of the dispersed pore-air in the soil pores results the increase of pneumatic pressure head in the soil profile. By reaching the pneumatic pressure of the pore-air to a critical pressure (according to Bouwer, 1966, the air entry value), the accumulated air breaks the weakest part of the soil body and escapes to the atmosphere. The soil profile after this stage can not be known as a confined one.

When the upper boundary of capillary zone coincides with the ground surface, the chance of exchange of place between air and water becomes great. In such cases the soil profile acts alternatively as a confining layer with regard to the air movement. Consequently, the formation of pore-air build-up is followed by the air escape from the soil profile. For this reason the pressure head in the layers close to the ground surface alternates very responsively and the discharge rate shows fluctuations. This fact was observed during *EXP. NO. 5*.

In the case of ponding infiltration, especially when ponding takes place instantly, most of the pore-air escapes in the form of bubbles at the beginning of ponding. After this stage the air in the soil pores remains in the dispersed form and can not become continuous because of the establishment of the water passage among the soil pores. In this context, Ishihara and Shimojima (1983) reported the discontinuity of infiltration process due to the intermittent pore-air escape. This holds true at the early stages of the ponding process.

6.2 Pore-air pressure effects at the open face of a subsurface flow system

The effect of pore-air pressure on the flow behavior of subsurface flow system was analyzed in Chapter V. In this section however, it is attempted to examine the above mentioned effects on the water content condition of the soil profile.

To analyze the condition of water content in the sand tank during *EXP. NO. 4*, at first, the pressure head at various parts of the sand tank were calculated from the recorded total potentials. Then these pressure head values were converted into water content using the water characteristic curve shown in Fig. 2.4. The results for the inlet zone, the middle and the outlet zone of the sand tank are shown in Fig. 6.1.

It is clear in this figure that the water content increases rapidly at the sand surface. But in the lower layers the increase of water content is slow until 430 minutes. As a consequent, after 430 minutes the water content profile shows an abrupt increase in the lower layers of the soil profile. If the water characteristic curve can closely estimate the water content condition of a soil profile when vertical flow is present, at this time a continuity in the water content is established in the whole soil profile at the outlet boundary. The delay in increase of water content in the lower layers of the sand tank demonstrates the effect of entrapped pore-air on the soil moisture formation. Moreover, Fig. 6.1 can demonstrate the remarkable effects of pore-air near the boundaries of the flow system where the movement of air is further restricted.

The evaluation of flux at the exit face of the sand tank further demonstrated that the vertical hydraulic gradient at the lower layer of the open face of the saturated capillary zone is close to the hydraulic gradients of the saturated zone. But in the upper layers, these hydraulic gradients are small. This observation coincides well with the results obtained by Gureghian (1981) under steady state.

6.3 Water table characteristics in the presence of vertical flow

In this section attempts have been made to examine the definition of the water table given by Lohman and others (1972) with the results of the *CPAP* and *UCPAP* ponding experiments (*EXPS. NO. 11* and *17*). For this purpose, the results of piezometric readings, the actual water table measurements and the atmospheric surfaces during these experiments are taken under consideration.

Lohman and others stated the water table as "the surface of an unconfined water body at which the pressure is atmospheric. It is defined by the level at which water stands in wells that penetrated the water body just far enough to hold standing water".

The piezometric surface at 30 minutes of the *CPAP* ponding experiment (*EXP. NO. 11*) shown in Fig. 5.1, lies higher than the atmospheric surface, but both are lower than the measured water table position. As the infiltration process continues, at 100 minutes of the experiment (Fig. 5.2), this difference decreases. Nevertheless, the atmospheric surface in this figure demonstrates different behavior than the observed water table position.

Furthermore, it is understood from this figure that except a small portion of the outlet boundary, the pressure head in the whole parts of the sand tank are positive. The appearance of water table in the form of atmospheric surface shown in the above mentioned figure creates the doubt that whether in actual circumstances a water table can be developed in such form. If this is the case, the measured water table in the observation wells behaves only as a piezometric surface in subsurface water phenomenon.

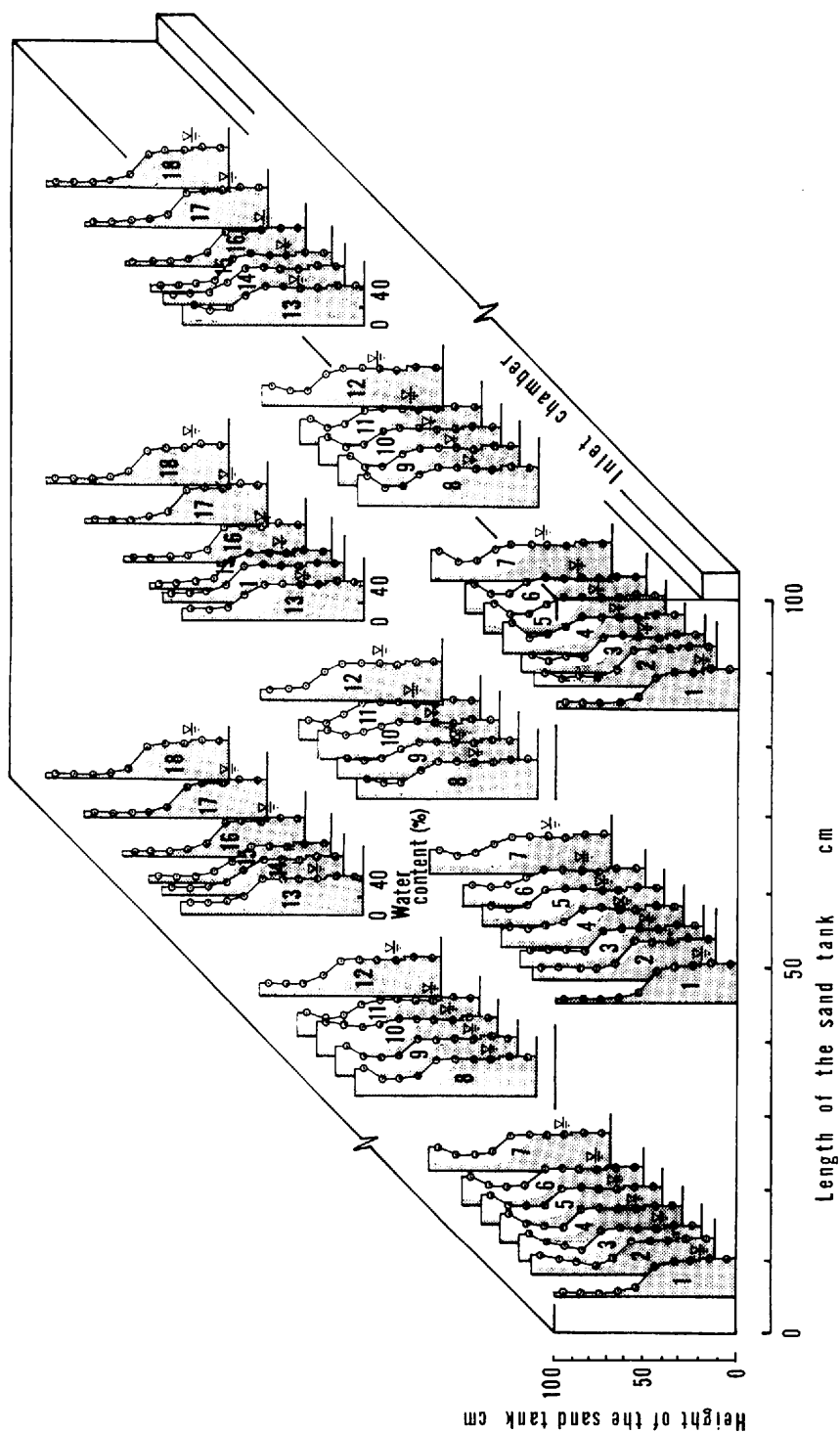


Fig. 6.1 Water content variations near the inlet, the middle and the outlet zone of the sand tank during EXP. NO. 4.

1 : t0;	2 : t35;	3 : t55;	4 : t85;	5 : t115;	6 : t145	7 : t197;	8 : t400;
9 : t430;	10 : t460;	11 : t490;	12 : t550;	13 : t880	14 : t910	15 : t930;	16 : t970;
17 : t1030;	18 : t1090.						
t35 :	Water content profile at 35 minutes.						

6.4 The significances of air and water entry values in subsurface flow

The air and water entry values of a soil profile play important roles in the soil water flow studies. But their physical behaviors have received the least attention in literature. The term "entry" is often interchanged in literature by the "threshold", "displacement", "bubbling pressure". However their magnitudes are the same.

Physically the air and water entry values coincide with the pressure head of the layer at which the capillarity is confronted with the atmospheric pressure in a soil profile. In chapter V it was observed that during an infiltration event, the entrapped pore-air in a soil profile can remain in the soil pores until its pressure head reaches the air entry value of that soil material. Corey (1977, p. 13) also related the pressure of the entrapped pore-air surrounded by the water in a soil pore equivalent to the air entry value, of that soil material.

Consequently the air entry value beside the other physical significances, shows the range of the soil particle distribution, the maximum pressure range that an entrapped pore-air can remain in a soil pore. Finally these values also indicate the pressure head of the soil profile above the water table in which the degree of saturation is close to the unity.

6.5 Problems to be studied further

In 1972, Philip in a review, documented the recent advances related with the soil water movement. Since then obviously great deal of developments related to the water movement in unsaturated soil have taken place. To be able to determine what are necessary for the future studies, such reviews are necessary to be done regularly.

In connection with this study, it is necessary to point out the problems that require further investigations.

- 1 – The advance of the wetting front cannot be estimated by using the unsaturated hydraulic conductivity values precisely.
- 2 – The behavior of water table in the existence of vertical flow requires extensive investigations.
- 3 – The physics of air and water entry values in subsurface flow studies are not yet analyzed in detail.
- 4 – Although in many subsurface flow studies the effect of temperature on the air and water movements are assumed negligible, it may influence strongly the above mentioned movements. Therefore detailed investigations are required concerning this subject.

CHAPTER VII

CONCLUSIONS

To elucidate the role of capillary zone in subsurface flow studies, laboratory experiments were performed in relation to the water table alteration and infiltration process. The results of the experiments are summerized as follows;

A – Due to the groundwater table alteration

- 1 – The saturated capillary zone acts as a siphon for water movement above the water table in response to the groundwater table alteration.
- 2 – The significance of capillary siphon flow is distinctive in places where the thickness of saturated zone is not great below the water table.

B – Due to the rainfall infiltration

- 3 – Among the other factors causing pulsation in subsurface flow aspects, entrapped pore-air is recognized as the distinguished and the remarkable one.
- 4 – The entrapped pore-air build-up significantly affects the discharge rate, the pressure head of the soil profile and the position of water table.
- 5 – The build-up of the entrapped pore-air in the soil profile continues as long as the pore-air pressure reaches the air entry value of the soil material. Subsequently, the pore-air escapes from the soil profile and thereafter the system acts as an unconfined one with respect to the pore-air pressure development.
- 6 – The flow of water movement in the vadose zone is vertical up to the upper boundary of the saturated capillary zone. Nevertheless as the water enters the capillary zone, its flow is diverted laterally toward the exit boundary of the flow system.
- 7 – The water and air entry values of the soil profile, and the location of water table from the ground surface carry significant importances in subsurface flow concept.

C – Due to the ponding infiltration

- 8 – The pressure head of the soil surface beneath the ponded water becomes positive soon after the ponding application, but it does not increase as long as the ponded water exists on the soil surface.
- 9 – The location of capillary zone from the ground surface governs strongly the infiltration rate into the soil.

ACKNOWLEDGEMENTS

The author wishes to express his sincere gratitudes to his academic advisor, Dr. I. Kayane, Prof. of the Inst. of Geoscience, for his guidance, encouragements and supports during the course of this study. His efforts for providing the author the opportunity of graduate studies in the University of Tsukuba and his kind treatments are heartily acknowledged.

Further thanks are due to Dr. M. Inokuchi, Dr. S. Takayama, Dr. S. Shindou, Dr. T. Nishizawa, Professors, Dr. K. Kotoda, and Dr. T. Sunamura, Associate Professors of the Inst. of Geoscience for their continuous supports and suggestions during the course of this research. Thanks are also due to Professor Dr. T. Kawamura, the director of the Environmental Research Center (*ERC*) of the University, for the permission of publication of this thesis as an *ERC* paper.

The author is grateful to Dr. T. Tanaka and Dr. Y. Suzuki, Lecturers of the Institute of Geoscience for their valuable comments, discussions and critical reading of the manuscript. Thanks are also due to Dr. A. Kondoh, the staff member of *ERC* for the helps and useful discussions. The author is further indebted to Dr. S. Yamamoto, former Prof. of the Rissho University, and Dr. H. Bouwer, the Director of U.S. Water Conservation Laboratory for their supports and encouragements.

Providing the permission of leave for this study by Dip. Eng. A. Sattar Oria, and Eng. Sheir M. Kamin, the President and the Vice President, respectively, of the Central Authority for Water Supply and Sewerage of Afghanistan is appreciated. The financial support of this research by the Ministry of Education, Science and Culture of Japanese Government is also acknowledged.

Furthermore, the models for this research were prepared in the Central Workshop and the Workshop of *ERC* of the University. Hence the cooperation of the staff members of the Central Workshop, and of the *ERC* are appreciated. The author is further grateful to Dr. A. Maekado, Dr. S. Nakagawa, Dr. M. Yasuhara, the former research assistant, Mr. T. Kojima, the former staff member of *ERC*, Mr. R. Suppiah, and the other colleagues in the University of Tsukuba for their assistance in various aspects of this study.

This thesis is dedicated to my parents, my teachers, my brothers and my children (Qawi and others) for their supports, encouragements and patience.

BIBLIOGRAPHY

- Adam, K. M., G. L. Bloomsburg, and A. T. Corey, (1969): Diffusion of trapped gas from porous media. *Water Resour. Res.*, **5**(4): 840-849.
- Akiba, M., (1938): The siphon action of sand and the induced capillary water. *J. Agric. Eng. Soc. Japan*, **10**: 147-157. (in Japanese)
- Alim, A. K., (1983): An experimental study on transient behavior of capillary fringe. *Unpublished Master thesis, Univ. of Tsukuba, Japan*, 151 pp.
- Alim, A. K., and I. Kayane, (1983): A laboratory experiment on the behavior of capillary zone using vertical columns. *Bull. Env. Res. Cen., Univ. Tsukuba, Japan*, **7**: 1-8. (in Japanese)
- Alim, A. K., and I. Kayane, (1985): Response of the capillary zone due to drying and wetting processes. *Sci. Rept., Inst. Geosci., Univ. Tsukuba, Japan, Sect. A*, **6**: 83-102.
- Anderson, D. M., and A. Linville, (1962): Temperature fluctuation at a wetting front: 1: Characteristic temperature-time curves. *Proc. Soil Sci. Soc. Amer.*, **26**: 14-18.
- Baver, L. D., (1956): "Soil Physics". Wiley, Modern Asia Ed., Tokyo, 489 pp.
- Bear, J., (1979): "Hydraulics of Groundwater". McGraw-Hill, New York, 567 pp.
- Bianchi, W. C., and Jr. E. E. Haskell, (1966): Air in the vadose zone as it affects water movements beneath a recharge basin. *Water Resour. Res.*, **2**(2): 315-322.
- Bouwer, H., (1964): Unsaturated flow in groundwater hydraulics. *Proc. ASCE., J. Hydraul. Div.*, **90**(HY5): 121-144.
- Bouwer, H., (1965): Theoretical aspects of seepage from open channels. *Proc. ASCE., J. Hydraul. Div.*, **91**(HY3): 37-59.
- Bouwer, H., (1966): Rapid field measurement of air entry value and hydraulic conductivity of soil as significant parameter in flow system analysis. *Water Resour. Res.*, **2**(4): 729-738.
- Bouwer, H., (1969): Infiltration of water into nonuniform soil. *Proc. ASCE., J. Irrig. Drain. Div.*, **95**(IR4): 451-462.
- Bouwer, H., (1978): "Groundwater Hydrology." McGraw-Hill, New York, 480 pp.
- Brooks, R. H., and A. T. Corey, (1964): Hydraulic properties of porous media. *Hydrol. Pap. 3, Colo. State Univ., Fort Collins*, 27 pp.
- Brutsaert, W. F., (1971): A functional iteration technique for solving the Richard's equation applied to two-dimensional infiltration problems. *Water Resour. Res.*, **7**(6): 1583-1596.
- Brutsaert, W. F., (1977): Vertical infiltration in dry soil. *Water Resour. Res.*, **13**(2): 363-368.
- Brustkern, R. L., and H. J. Morel-Seytoux, (1970): Analytical treatment of two-phase infiltration. *Proc. ASCE., J. Hydraul. Div.*, **96**(HY12): 2535-2548.
- Cedergren, H. R., (1977): "Seepage, Drainage and Flow Nets." Wiley-Interscience, New York, 534 pp.
- Chapman, T. G., (1960): Capillary effects in a two-dimensional groundwater flow system. *Geotechnique J.*, **10**: 55-61.
- Childs, E. C., (1967): Soil moisture theory. *Advances in Hydrosol.*, V. T. Chow (Ed.), **4**: 73-17.
- Childs, E. C., (1969): "An Introduction to the Physical Basis of Soil Water Phenomena." Wiley Interscience, New York, 493 pp.
- Chu, S. T., (1978): Infiltration during an unsteady rainfall. *Water Resour. Res.*, **14**(3): 461-466.
- Collis-George, N., (1977): Infiltration equations for simple soil systems. *Water Resour. Res.*, **13**(2): 395-403.
- Corey, A. T., (1977): "Mechanics of Heterogeneous Fluids in Porous Media." Water Resour. Publications, Fort Collins, Colo., 259 pp.

- Debacker, L. W., (1967): The measurement of entrapped gas in the study of unsaturated flow phenomena. *Water Resour. Res.*, 3(1): 245-249.
- Dixon, R. M., (1976): Comments on "Derivation of an equation of infiltration" by Morel-Seytoux and Khanji. *Water Resour. Res.*, 12(1): 116-118.
- Dixon, R. M., and D. R. Linden, (1972): Soil air pressure and water infiltration under border irrigation. *Proc. Soil Sci. Soc. Amer.*, 36: 948-952.
- Dunne, T., and L. B. Leopold, (1978): "*Water in Environmental Planning*." W. H. Freeman, San Francisco, 818 pp.
- Freeze, R. A., (1969): The mechanism of natural groundwater recharge and discharge. 1. One-dimensional, vertical, unsteady, unsaturated flow above a recharging or discharging groundwater flow system. *Water Resour. Res.*, 5(1): 153-171.
- Freeze, R. A., (1971): Three-dimensional, transient, saturated-unsaturated flow in a groundwater basin. *Water Resour. Res.*, 7(2): 347-366.
- Freeze, R. A., and J. A. Cherry, (1979): "*Groundwater*" Prentice-Hall, Englewood Cliffs, N. J., 604 pp.
- Green, W. H., and G. A. Ampt, (1911): Studies on soil physics: I. The flow of air and water through soils. *J. Agric. Sci.*, 4: 1-24.
- Gureghian, A. B., (1981): A two-dimensional finite element scheme for the saturated-unsaturated flow with applications to flow through ditch drained soils. *J. Hydrol.*, 50: 333-353.
- Heath, R. C., (1983): "*Basic Groundwater Hydrology*." U. S. Geol. Surv., *Water Supply Pap.* 2220, U.S. Government printing office, 84 pp.
- Horton, J. H., and R. H. Hawkins, (1965): Flow path of rain from soil surface to the water table. *Soil Sci.*, 100(6): 377-383.
- Ishihara, Y., and E. Shimojima, (1983): A role of pore air in infiltration process. *Bull. Disaster Prevention Res. Inst., Kyoto Univ.*, 33: 163-222.
- Kirkham, Don., (1967): Explanation of paradoxes in Dupuit-Forchheimer seepage theory. *Water Resour. Res.*, 3(2): 609-622.
- Knapp, B. J., (1978): Infiltration and storage of soil water. In "*Hillslope Hydrology*," M. J. Kirkby (Ed.), Wiley-Interscience, 389 pp.
- Lohman, S., and others, (1972): Definitions of selected groundwater terms-Revisions and conceptual refinements. *U.S. Geol. Surv., Water Supply Pap.* 1988, 21 pp.
- Luthin, J. N., (1969): Some observations on flow in the capillary fringe. In "*Flow in Unsaturated Zone*," UNESCO, Paris, 905-909.
- McWhorter, D. E., (1971): Infiltration affected by flow of air. *Hydrol. Pap.* 49. Colo. State Univ., Fort Collins, 43 pp.
- McWhorter, D. B., and D. K. Sunada, (1977): "*Groundwater Hydrology and Hydraulics*." Water Resour. Publication, Fort Collins, Colo., 290 pp.
- Mein, R. G., and C. L. Larson, (1973): Modeling infiltration during a steady rain. *Water Resour. Res.*, 9(2): 384-394.
- Morel-Seytoux, H. J., (1978): Derivation of equations for variable rainfall infiltration. *Water Resour. Res.*, 14(4): 561-568.
- Morel-Seyoux, H. J., and J. Khanji, (1974): Derivation of an equation of infiltration. *Water Resour. Res.*, 10(4): 795-800.
- Morel-Seytoux, H. J., T. A. Pick, and J. C. Torkil, (1977): Computation of infiltration for unsteady uninterrupted high rainfall. *J. Hydrol.*, 35: 221-234.

- Muskat, M., (1937): "*The Flow of Homogeneous Fluids Through Porous Media*." McGraw-Hill, 763 pp.
- Neuman, S. P., (1976): Wetting front pressure head in the infiltration model of Green and Ampt. *Water Resour. Res.*, **12**(3): 564-566.
- Noblanc, A., and H. J. Morel-Seytoux, (1972): Perturbation analysis of two-phase infiltration. *Proc. ASCE., J. Hydraul. Div.*, **98**(HY9): 1527-1541.
- Parlange, J. Y., (1975): A note on the Green and Ampt equation. *Soil Sci.*, **119**(6): 466-467.
- Parlange, J. Y., and D. E. Hill, (1979): Air and Water movement in porous media: Compressibility effect. *Soil Sci.*, **127**(5): 257-263.
- Peck, A. J., (1965a): Moisture profile development and air compression during water uptake by bounded porous bodies: 2. Horizontal column. *Soil Sci.*, **99**(5): 327-334.
- Peck, A. J., (1965b): Moisture profile development and air compression during water uptake by porous bodies: 3. Vertical column. *Soil Sci.*, **100**(1): 44-51.
- Perrens, S. J., and K. K. Watson, (1977): Numerical analysis of two-dimensional infiltration and redistribution. *Water Resour. Res.*, **13**(4): 781-790.
- Philip, J. R., (1957a): The theory of infiltration: 1. The infiltration equation and its solution. *Soil Sci.*, **83**: 345-357.
- Philip, J. R., (1957b): The theory of infiltration: 2. The profile of infinity. *Soil Sci.*, **83**: 435-448.
- Philip, J. R., (1957c): The theory of infiltration: 3. Moisture profile and relation to experiment. *Soil Sci.*, **84**: 163-178.
- Philip, J. R., (1957d): The theory of infiltration: 4. Sorptivity and algebraic infiltration equations. *Soil Sci.*, **84**: 257-264.
- Philip, J. R., (1958): The theory of infiltration: 7. *Soil Sci.* **85**: 333-337.
- Philip, J. R., (1959a): Energy dissipation during absorption and infiltration: 1. *Soil Sci.*, **86**: 132-136.
- Philip, J. R., (1959b): Energy dissipation during absorption and infiltration: 2. *Soil Sci.*, **86**: 353-358.
- Philip, J. R., (1969): Theory of infiltration. In "*Advances in Hydrosience*" V. T. Chow (Ed.), **5**: 215-305.
- Philip, J. R., (1972): Future problems of soil water research: *Soil Sci.*, **113**(4): 294-300.
- Rennolls, K., R. Carnell, and V. Tee, (1980): A descriptive model of the relationship between rainfall and soil water table. *J. Hydrol.*, **47**: 103-114.
- Richards, L. A., (1931): Capillary conduction of liquids through porous mediums. *Phys.*, **1**: 318-333.
- Rodda, J. C., R. A. Downing, and F. M. Law, (1976): "*Systematic Hydrology*." Newness-Butterworth, London.
- Rubin, J., and R. Steinhardt, (1963): Soil water relations during rain infiltration: 1. Theory. *Soil Sci. Soc. Amer. Proc.*, **27**: 246-251.
- Rubin, J., R. Steinhardt and P. Reiniger, (1964): Soil water relations during rain infiltration: II. Moisture content profiles during rains of low intensities. *Soil Sci. Soc. Amer. Proc.*, **28**: 1-5.
- Schmid, P., and J. Luthin, (1964): The drainage of sloping lands: *J. Geophysical Res.*, **69**(8): 1525-1529.
- Sklash, M. G., and R. N. Farvolden, (1979): The role of groundwater in storm runoff. *J. Hydrol.*, **43**: 45-65.
- Stephens, D. B., and S. P. Neuman, (1982): Free surface and saturated-unsaturated analysis of borehole infiltration tests above the water table. *Advances in Water Resour.*, **5**: 111-116.
- Swartzendruber, D., (1974): Infiltration on constant-flux rainfall into soils as analyzed by the approach of Green and Ampt. *Soil Sci.*, **117**(5): 272-281.
- Tanaka, T., M. Yasuhara and A. Marui (1982): Pulsating flow phenomena in soil pipe. *Ann. Rep. Inst. Geosci., Univ. Tsukuba*, **8**: 33-36.
- Touma, J., G. Vachaud, and J. Y. Parlange, (1984): Air and water flow in a sealed, ponded vertical soil Column. Experiment and model. *Soil Sci.*, **137**(3): 181-187.

- Vachaud, G., and J. L. Thony, (1971): Hysteresis during infiltration and redistribution in a soil column at different initial water content. *Water Resour. Res.*, **7**(1): 111-127.
- Vachaud, G., J. P. Gaudet, and V. Kuraz, (1974): Air and water flow during ponded infiltration in vertical bounded column of soil. *J. Hydrol.*, **22**: 89-108.
- Vachaud, G., M. Vauclin, D. Khanji, and M. Wakil, (1973): Effects of air pressure on water flow in an unsaturated stratified vertical column of sand. *Water Resour. Res.*, **9**(1): 160-173.
- Vauclin, M., D. Khanji, and G. Vachaud, (1979): Experimental and numerical study of a transient, two-dimensional unsaturated-saturated water table recharge problem. *Water Resour. Res.*, **15**(5): 1089-1101.
- Verruijt, A., (1970): "*Theory of Groundwater Flow*." Macmillan, London. 190 pp.
- Warrick, A. W., D. O. Lomen, and S. R. Yates, (1985): A generalized solution to infiltration. *Soil Sci. Soc. Amer. Proc.*, **49**: 34-38.
- Weeks, E. P., (1978): Field determination of vertical permeability of air in the unsaturated zone. *U.S. Geol. Surv., Professional Pap.* **1051**, 41 pp.
- Willard, A. M. and P. L. Monkmeyer, (1973): Validity of Dupuit-Forchheimer equation. *Proc. ASCE., J. Hydraul. Div.* **99**(HY9): 1573-1582.
- Wilson, L. G., and J. N. Luthin, (1963): Effect of air flow ahead of wetting front on infiltration. *Soil Sci.* **96**: 136-143.
- Youngs, E. G., and A. J. Peck, (1964): Moisture profile development and air compression during water uptake by bounded porous bodies: 1. Theoretical introduction. *Soil Sci.*, **98**: 290-294.

Environmental Research Center Papers

- No. 1 (1982) Kenji KAI: Statistical characteristics of turbulence and the budget of turbulent energy in the surface boundary layer. 54p.
- No. 2 (1983) Hiroshi IKEDA: Experiments on bedload transport, bed forms, and sedimentary structures using fine gravel in the 4-meter-wide flume. 78p.
- No. 3 (1983) Yousay HAYASHI: Aerodynamical properties of an air layer affected by vegetation. 54p.
- No. 4 (1984) Shinji NAKAGAWA: Study on evapotranspiration from pasture. 87p.
- No. 5 (1984) Fujiko ISEYA: An experimental study of dune development and its effect on sediment suspension. 56p.
- No. 6 (1985) Akihiko KONDOH: Study on the groundwater flow system by environmental tritium in Ichihara region, Chiba Prefecture. 59p.
- No. 7 (1985) Chong Bum LEE: Modelling and climatological aspects on convective boundary layer. 63p.
- No. 8 (1986) Kazuo KOTODA: Estimation of river basin evapotranspiration. 66p.
- No. 9 (1986) Abdul Khabir ALIM: Experimental studies on transient behavior of capillary zone. 76p.

発行

昭和61年3月25日

編集・発行者 筑波大学水理実験センター

〒305 茨城県新治郡桜村天王台1-1-1

TEL 0298 (53) 2532

印刷 日青工業株式会社

〒105 東京都港区西新橋2-5-10